Journal of Industrial and Engineering Chemistry 119 (2023) 550–573

Contents lists available at ScienceDirect

Journal of Industrial and Engineering Chemistry

journal homepage: www.elsevier.com/locate/jiec

Esterification of stearic acid using novel protonated and crosslinked amidoximated polyacrylonitrile ion exchange fibres

Rawaz.A. Ahmed, Sanaa Rashid, Katherine Huddersman *

School of Pharmacy, Faculty of Health and Life Sciences, De Montfort University, The Gateway, Leicester LE1 9BH, UK

ARTICLE INFO

Article history:
Received 29 August 2022
Revised 21 November 2022
Accepted 1 December 2022
Available online 15 December 2022

Keywords:
Fats Oil and Greases (FOGs)
Free fatty acids (FFAs)
Esterification reaction
Methyl ester
Amidoxime modified Polyacrylonitrile (PANF)

ABSTRACT

This study will demonstrate the conversion of stearic acid to methyl stearate (biodiesel) using for the first time crosslinked amidoximated polyacrylonitrile ion-exchanged mesh protonated by sulphuric acid. Quantitative analysis of conversion was by GC-FID, ^{1}H NMR and ATR-FT-IR with GC-FID the most reliable. A molar ratio of methanol to stearic acid of 35.5: 1 gave 94 % conversion to the ester at 90 °C. At 65 °C and a greater ratio of 87.1:1 conversion was 94.1 % comparable to the 98 % yield obtained with 1wt% H_2SO_4. Re-use at 65 °C gently dropped to 57 % on the 13th cycle. Regeneration by washing with dichloromethane and re-acidification achieved 84 % conversion but quickly deactivated due to blocking of sites by methyl stearate as shown by ATR-FTIR. This protonated amidoxime PAN catalyst (distinct from sulfonated fibres) exhibited higher stability than other heterogeneous protonated catalysts (ion-exchange resins, zeolites, clays) used lower temperatures and shorter reaction times. Advantages of using a mesh in place of powders are its ease of removal/replacement for continuous flow reactors promoting quick changes in process parameters. This study is promising as providing a sustainable protonated catalyst for use in converting Fats, Oils and Greases (FOG's) in waste oils and wastewater to biodiesel.

Introduction

Bio-fuel has been identified globally as an alternative fuel source to replace diesel fuel currently derived from fossil sources [1]. Among liquid renewable energy, biodiesel can be used in diesel engines without the need for modification [2]. Biodiesel is a fuel produced by chemically reacting lipids such as animal fat (tallow) or some other vegetable oils with an alcohol producing methyl, ethyl, or propyl esters [3,4] FOGs (fats, oils and greases) are lipid-rich waste from restaurants or in wastewater that can be considered as a potential low cost and abundant feedstock [1,3,5,6]. A recent analysis of brown grease (discharged into the sewer system) contained "60 % FOGs, 25 % water, and 15 % biosolids by mass" as suggested in Ahmed and Huddersman, 2022 [3,7]. Direct discharge of FOGs from housing can clog up the pipes which can ultimately result in property flooding due to sanitary sewer overflows (SSO) [3].

In recent years, many sewage blockages have globally been attributed to FOGs, for example in the US with an estimated cost of about US$ 25 billion for removal of sewer blockages per year [8]. Thus, FOGs discharge is a global issue which requires immediate management and due to growing populations and urbanization, this will only increase. Although some measures have been put in place, no sustainably effective treatments have so far been implemented. A solution to this growing problem is to develop technology to convert waste FOGs to renewable biodiesel energy [3]. Wastewater containing Fats, Oils, and Greases (FOGs) are among the least studied types of renewable liquid feedstocks for biodiesel production. In the few papers that have looked at the conversion of Fats, Oils, and Greases (FOGs) as they occur in wastewater into biofuel (biodiesel) via transesterification and esterification reactions (See Scheme 1 and 2) some success has been shown [3,8,9,10]. Since transesterification and esterification are both equilibrium reactions, to achieve a good conversion of free fatty acids (FFA) as well as the triglyceride (TG), the molar ratio of alcohol/oil should be increased above the stoichiometric amount [3].

However, traditional transesterification processes utilizing homogeneous base protonated catalysts such as NaOH or KOH are ill suited for processing FOG feedstocks. This is due to the high content of free fatty acid (FFA) and moisture in the FOGs, arising from biological activity [3]. These FFAs cause saponification during the transesterification reaction and hence, a lower yield of esters. To overcome this situation, acid protonated catalysts are used to

* Corresponding author.
E-mail address: huddzeo1@dmu.ac.uk (K. Huddersman).

https://doi.org/10.1016/j.jiec.2022.12.001

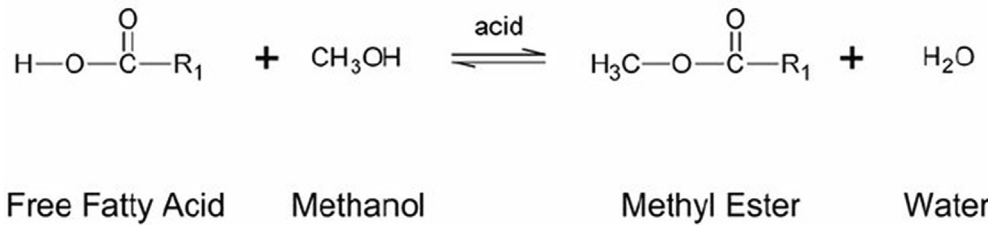

Scheme 1. Esterification reaction for biodiesel synthesis [3,9,10] where R1 denotes any hydrocarbon chain.

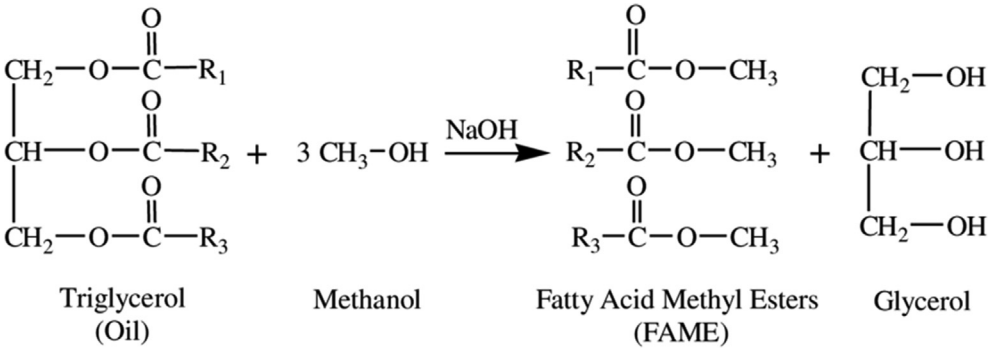

Scheme 2. Transesterification reaction for biodiesel synthesis [9,10]. Where R_1, R_2, R_3 denotes any hydrocarbon chain [3].

reduce the free fatty acid content by esterification before the transesterification process [3]. Strong acid protonated catalysts, such as H_2SO_4, HCl, HI are less sensitive to the influence of free fatty acids which allows them to esterify and transesterify low quality feedstocks simultaneously [3,7,11].

Esterification is an essential industrial process used in food, pharmaceutics industries, as well as, for the production of biofuels. Many researchers have focused on transforming free fatty acid oily feedstocks via two steps; firstly, to esterify free fatty acids into fatty acid methyl ester (FAME), that is, biodiesel and secondly to trans-esterify triglyceride to the FAME product. Therefore, homogenous catalysis of the esterification process has been well established for biodiesel production [9,11,12,13,14]. For example; Al-Arafi N. using sulfuric acid as well as three other homogeneous acidic catalysts, investigated the esterification of oleic acid with oleyl alcohol to yield the wax ester oleyl oleate [15], using the following optimum conditions: reaction time of 5 h, temperature 90 °C, 1.25 wt.% of protonated catalyst and molar ratio of oleyl alcohol to oleic acid of 1:1 [15] to result in 93.88 % conversion to the ester. Out of the four catalysts in Al-Arafi's study, sulfuric acid showed relatively higher specific activity as compared to phosphoric acid, perchloric acid and p-toluene sulfonic acid (p-TSA) catalysts, which gave 52.7 %, 54.9 % and 70 % yield of FAMEs, respectively [15]. In another study, naphthenic acid was esterified in a batch reactor using sulfuric acid (H_2SO_4) to give a yield of 95 % of methyl naphthenate with optimum reaction conditions: molar methanol to acid ratio 14:1, reaction temperature 80 °C, 0.7 wt.% of H_2SO_4 for 6 hours [16]. Current work on the esterification of tall oil fatty acid in homogenous catalysis using sulfuric acid gave a yield of FAME of 96.76 % with a methanol to oil molar ratio of 15:1, 0.5 wt.% H_2SO_4, reaction temperature 55 °C for 60 min [17]. These protonated catalysts, such as, sulphuric acid are however, non-renewable, and give rise to difficulties, such as, the corrosion of equipment, transportation problems, waste generation and environmental problems. Therefore, current research for the production of biodiesel is focused on renewable Solid Acid Protonated catalysts (SACs). Recently, interest has been growing into the use of heterogeneous protonated catalysts because of their low cost, ease of use and environmental friendliness. Varieties of heterogeneous protonated catalysts have been used in long chain acid esterification. These include ZrO_2/SiO_2 [18], zeolites [19], Amberlyst 70 [20], Amberlyst-15 [21], Amberlyst 46 resin [22], Amberlyst- 15 ion exchange resin [23]. Table 1 shows the list of heterogenous acid protonated catalysts with optimum conditions for esterification of free fatty acids (FFAs).

The protonated heterogeneous acid catalysts in the literature are powders or resin microbeads used in batch reactions and are not easily suitable for continuous flow production in industry. To fill this gap in the state-of the art we have developed a self-supporting fibrous mesh with excellent hydrodynamic properties that is easy to replace and is suitable for continuous flow production and which can be modified to act as an acid catalyst. The De Montfort University ion exchange fibrous PANF mesh contains amidoxime groups but does not possess acidic properties and has of yet not been investigated for esterification reactions. Nevertheless, with suitable acid treatment, it can be protonated and used as an acid catalyst for the esterification process. 2 M H_2SO_4 acid was used to modify the PANF to obtain protonated amidoxime groups in contrast to the sulphonated polymers (sulphonation is when there is a chemical bond between a carbon atom of the polymer and the sulphur of the sulphonic acid group) which comprise most of the heterogeneous solid acid catalysts. The amidoxime PAN ion exchange fibres were obtained by modification of the cyano-group with a mixture of hydrazine sulphate and hydroxylamine sulphate at pH 9.5 at 95 °C to produce a crosslinked polymer containing amidoxime groups [24]. The main novelty of the present work is the production of the sulfuric acid treated fibrous PANF amidoxime ion exchanger (hereafter called the protonated catalyst) in the format of a mesh for the esterification process with optimization of the experimental parameters such as temperature, molar ratio between fatty acids and alcohol, amount of acidified ion exchanger, reaction time, and catalyst reusability. This work is highly original as there has been no use of this fibrous supported catalyst for biodiesel production and very little use of any fibrous acid catalyst. The fibrous mesh is much easier to handle than powdered catalysts which also suffer from back pressure. The protonated mesh can be

Table 1
List of heterogenous acid protonated catalysts with optimum conditions for esterification of FFAs. Reproduced from Ahmed and Huddersman, 2022 [3].

FFA	Protonated catalyst	Reaction condition	Yield %	Ref
Stearic acid	Mesoporous ZrO_2/SiO_2 protonated catalysts prepared with cationic (CTAB) and non-ionic surfactants.	0.4 g cat., 3hr, ethanol/stearic acid molar ratio of 120:1, 120 °C	76.9 % which reduced to 72.5 %after five cycles,	[18]
Stearic acid	Iron Exchanged Montmorillonite (Fe-MMT K10) protonated catalyst	2 g of SA, 100 ml methanol,80 °C for 3 h,600 mg of solid cat	68 %, ethanol 78 % methanol	[25]
Stearic acid	PA/NaY (PA = organophosphonic acid, NaY = Na exchanged zeolite Y protonated catalyst	2.0 g cat., 4 h, molar ratio of alcohol to acid. 4:1, 95 and 100 °C.	69.10 %	[26]
Oleic acid	Co-Ni-Pt/ FAU-type zeolite protonated catalyst	Ethanol to oleic acid molar ratio 6:1, 70 °C, 1.5–2 h, batch, and continuous	93 %- batch and 89 %- continuous	[19]
Lauric acid -PFAD	Ammonium ferric sulphate-calcium silicate AFS-CS protonated catalyst	Methanol to lauric acid or Palm fatty acid distillate (PFAD) molar ratio 15:1, 65 °C, 2 h, 16 % AFS-CS,	−100 % for LA −72.6 % for (PFAD)	[11]
Oleic acid	1-methylimidazolium hydrogen sulfate, $[HMIM]HSO_4$, ionic liquid	methanol/oleic acid molar ratio = 15:1, 8 h, 110 ± 2 °C, 15 wt.% cat.	95 % 90 %	[27]
Oleic acid	Zinc acetate	Molar ratio of methanol to oleic acid 4:1, 1 0.0 wt.% zinc acetate, 6.0 MPa & 220 °C.	95 %	[28]
Myristic acid	Sulfated zirconia (SZ) solid acid protonated catalyst	Myristic acid to methanol molar ratio of 1:10, 0.5 wt.% cat. 5 h.	98 %, after five cycles reduced to 87 %	[29]
Palmitic acid	H-Y and ZSM-5 zeolites as solid acid protonated catalysts	Methanol to palmitic acid molar ratio 2:1, 3 μmol of cat., at 70 °C, 3 h.	100 %, possibly recyclable	[30]
Oleic acid	10 % and 20 % WO_3/USY zeolites	Methyl acetate to oleic acid molar ratio 10:1, 10 %, 20 % cat., 240 °C,	79.4 wt.% and 80.8 wt.%	[31]
Lauric acid	Ag_1 $(NH_4)_2PW_{12}O_{40}$/UIO-66	Lauric acid to methanol molar ratio 1:15, 10 wt. % cat., 150 °C,3h	75 %, reduced to 58 % on sixth recycle	[32]
Stearic, oleic, palmitic acids	Montmorillonite-based clay protonated catalysts (KSF, KSF/0, KP10, and K10)	2 g of FFA, in the presence of 0.2 g KSF/0 (Protonated catalyst 0.1w/w) at 150 °C	97 %, 84 % after three cycles).	[33]
Lauric acid	Niobic acid, niobium phosphate	FA (50 mmol), alcohol (500 mmol), 10wt. % cat, 120–160 °C, 7 h.	97 %, no loss of activity after 3 cycles	[34]

used in continuous flow where it is easier to change reaction conditions during production and a smaller reactor can be used than in batch with considerable reduction in both footprint and capital costs. We suggest that the acid catalyst mesh has potential in esterification of FFAs and hence would be useful in biodiesel production from low value waste sources such as FOGs.

Experimental work

Chemical materials

The PAN mesh was modified with dihydrazine sulphate (Aldrich with purity > 98 %), and hydroxylamine sulphate (99 %, Aldrich). The functionalised PANF mesh was acidified using sulfuric acid (98 %, Aldrich).

Fatty acid: Oleic acid, (90 %, Fisher Scientific), Stearic acid (97 %, Aldrich), Palmitic acid (98 %, Fischer Scientific). Methyl Ester of Fatty Acid: Methyl Oleate (99 %, Fisher Scientific, Analytical Standard), Methyl palmitate (95 %, Fischer Scientific), Methyl stearate (99 %, Fischer Scientific). Toluene (≥99.7 % GC), Methanol (99.8 % GC), Dichloromethane (≥99.9 %, GC), Hexane (95 % N-Hexane, Fisher Scientific), Chloroform-D (99.8 % + 0.05 % TMS).

Preparation of the surface functionalized amidoxime PAN fibres

The polyacrylonitrile ion exchanger (92 % PAN and 8 % vinyl acetate) are in the form of a mesh which contains approximately 50 % PAN yarn fibres and 50 % polypropylene monofilament and is made on an industrial scale, though it is not currently commercially available and is prepared by modification of the cyano-group of the PANF [24]. Modification solutions were prepared from a dihydrazine sulphate and hydroxylamine sulphate solution at pH 9.5 with heating at 95 °C for two hours. It was then treated with alkali at pH 12 at 60 °C for 15 minutes followed by washing with water and then dried. The functionalized amidoxmated PAN fibres are acidified at ambient temperature for 24 hr with 2 M H_2SO_4 to convert the groups to their protonated form and then dried.

Esterification reaction

Esterification of stearic acid with methanol was carried out in a liquid phase batch reactor. Stearic acid (1 g), with varying amounts of methanol and protonated catalyst (acidified at ambient temperature with 2 M H_2SO_4) were placed in a round bottom flask in a Radley carousel. Both stearic acid and methanol were preheated separately at a temperature 60–70 °C, then pre-heated methanol was gently added into the melted stearic acid after which the acidified PANF mesh solid catalyst was added followed by mixing. The solution phase had a total volume of 26–27 ml for all experiments except the kinetic runs. The reactant mixture was magnetically stirred and heated under water reflux (See Photo 1). After the reaction completed, the solution phase was poured into another container and hence PANF heterogenous catalyst was easily separated from the reaction mixture. The reaction mixture was slowly evaporated for 1-2hr by rotary evaporator at 45–55 °C to evaporate the excess methanol and water. After cooling to room temperature, the solidified product contained methyl stearate (m.pt. 34–40 °C) and unreacted stearic acid (m.pt. 67–70 °C).

In order to determine the effect of different process parameters, the amount of protonated catalyst, molar ratios of FFA to methanol, reaction time and temperature were studied. To determine the extent to which the protonated catalyst could be recycled after each reaction the protonated catalyst was removed and put into fresh feed. All esterification reactions were repeated twice with 0.2–10 % error, whilst the averaged data of the two reactions were used to plot the results in the Figures below. The kinetic study experiments were also performed, with methanol to acid molar ratio 87.7:1 at temperatures ranging from 45 °C to 75 °C with 6 g of protonated catalyst. The total volume of the reaction mixture for the kinetic study was increased to 109.52 ml to reduce error percentage below 10 % on the removal of 1 mL of sample for analysis at each time point resulting in a total removal of 6 mL over the 120 min of the esterification reaction. All esterification reactions were carried out in duplicate with the differences between the duplicate reactions shown by error bars in the figures.

Preparation of standards

Quantitative analysis of fatty acid methyl esters was performed by GC-FID (Thermofisher GC (TRACE1310)). 5–10 mg of each standard was dissolved in 10–20 ml of toluene and ultrasonicated at 50–55 °C for 25–30 min. Calibration plots of the individual fatty acid methyl esters were determined for concentrations within the ranges as follows: methyl stearate and methyl palmitate 78–2500 ppm, and methyl oleate 80–2570 ppm. Triplicate injections were performed for each standard solution to give standard deviations and a correlation coefficient (r^2) not less than 0.999, thus confirming the linearity of the method (Table 2).

A calibration curve for the quantitative analysis by ATR-FTIR was obtained using known concentrations of the fatty acid and methyl ester and noting their peak heights [35–37]. The sample preparation for ATR-FTIR were performed by grinding the stearic acid and methyl stearate (FAME) standards to make very fine powders in a pestle and mortar for 10 min. A calibration curve was obtained using known concentrations of mixtures of the fatty acid and methyl ester and noting their peak heights [35–37]. A calibration of % mass of the model methyl ester compound in six mixtures of methyl ester and fatty acid model compounds was plotted against absorbance as shown in Table 2. Five absorbance measurements (peak height) were taken for each standard mixture and the average of absorbance vs % mass had a Standard Deviation (SD) as in Table 2 and the correlation coefficient for the calibration plots obtained were not less than r2 = 0.999.

Characterization technique

GC-FID analysis was conducted using a Thermofisher GC (TRACE1310), equipped with a flame ionization detector (FID) and manual sampler. 5–10 mg of the solid product was re-dissolved in 10–20 ml of toluene and ultrasonicated at 50–55 °C for 25–30 min after which the samples were analyzed via GC-FID and the peak areas used for quantification. Sample aliquots of 1 μl were injected using a spilt mode of (40:1) with both the injector and detector temperatures held at 250 °C. Hydrogen was used as carrier gas at constant flow (2.4 ml/min). Chromatographic separation was performed using a Nitroterephthalic Acid Modified Polyethylene Glycol capillary column (Zebron ZB-FFAP, GC Column (60 m × 0.25 mm × 0.25 μm,). The oven temperature was set at 200 °C and increased at a rate of 4 °C/min up to 260 °C. Injections were performed in triplicate to obtain SD for the analysis.

^{1}H NMR analyses were conducted using a JEOL ECZ 600 MHz spectrometer operating at 200–300 MHz. The solvent used was deuterated chloroform $CDCl_3$ (Chloroform-D 99.8 % + 0.05 % TMS). Chemical shifts (δ) were expressed in parts per million (ppm), and the values of the coupling constant (J) were expressed in Hertz (Hz). Conversion percentage (C, %), by ^{1}H NMR was calculated according to equation (1) given in the literature [13,38].

$$Conversion\% = \frac{2A_{EM}}{3A_{CH2}} * 100 \quad (1)$$

A_{EM} is the integration value (area)of the hydrogens from the methoxy group in the methylesters $(3.6 - 3.7\ ppm)$

A_{CH2} is the integration value (area)of the methylene hydrogens in position α − to carbonyl $(2.25 - 2.3\ ppm)$

All the esterification products and the model stearic acid and methyl stearate were analysed by ^{1}H NMR in order to determine the conversion of the stearic acid into fatty acid methyl esters (equation (1)). Only the signals relating to the hydrogens from

Table 2
GC-FID and ATR-FT-IR calibrations for standard fatty acid methyl esters.

Quantitative analysis of FAMEs based on GC-FID.					
No.	FAME conc. ppm	Av. RT	±SD	Av. Peak Area	±SD
Methyl stearate with R^2 = 0.9998					
1.	78	9.78	0.0051	0.33	0.016
2.	156	9.78	0.0036	0.68	0.027
3.	312	9.79	0.0025	1.41	0.059
4.	625	9.80	0.0017	2.95	0.030
5.	1250	9.81	0.0006	6.17	0.040
6.	2500	9.82	0.0036	12.71	0.028
Methyl palmitate with R^2 = 0.9999					
1.	78	7.52	0.0011	0.3498	0.0024
2.	156	7.52	0.0029	0.7097	0.0006
3.	312	7.53	0.0011	1.3811	0.0066
4.	625	7.53	0.0026	2.823	0.039
5.	1250	7.54	0.0017	5.689	0.065
6.	2500	7.55	0.00	11.576	0.0056
Methyl Oleate with R^2 = 0.9998					
1.	80.	10.27	0.35	0.318	0.0016
2.	160	10.08	0.005	0.650	0.0076
3.	321.	10.08	0.003	1.361	0.0186
4.	642	10.08	0.004	2.876	0.0809
5.	1285	10.09	0.003	5.923	0.0770
6.	2570	10.10	0.003	12.137	0.137
Quantitative analysis of methyl stearate based on ATR-FTIR tools					
Absorbance peak position at 1750–1700 cm^{-1} with R^2 = 0.999					
No.	[m/m%]	Av. Absorbance		± SD	
1.	0 %	0		-	
2.	25 %	0.09		0.00049	
3.	55 %	0.202		0.00075	
4.	65 %	0.243		0.00064	
5.	85 %	0.318		0.00075	
6.	100 %	0.39		0.00414	

Av. = average of data, [m/m%] = [mass of methyl stearate / total mass (mass of stearic acid + mass of methyl stearate)] *100.

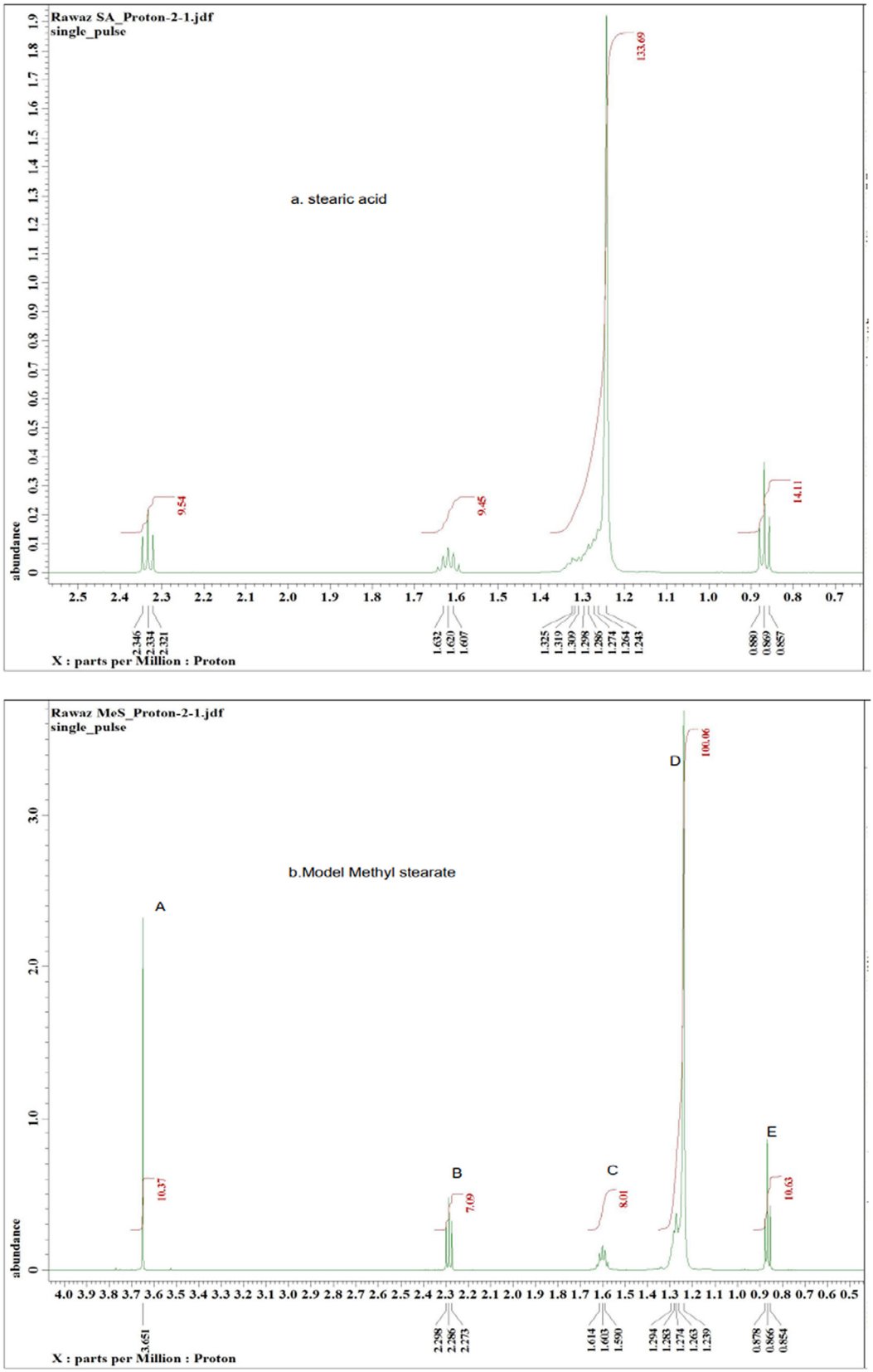

Fig. 1. A typical 1H NMR spectrum of the model compounds a) stearic acid and b) methyl stearate with labelling of the major peaks.

the methoxy group in FAMEs (singlet, 3.60–3.70 ppm) and the methylene hydrogens in position α- to the carbonyl (triplet, 2.24–2.29 ppm) were used for the quantification.

Fourier transform infrared (ATR-FTIR) analysis was performed using an ATR-FT-IR (Bruker Alpha Platinum ATR-FTIR) in the range 400–4000 cm^{-1} with resolution of 1 cm^{-1}. Approximately 20–

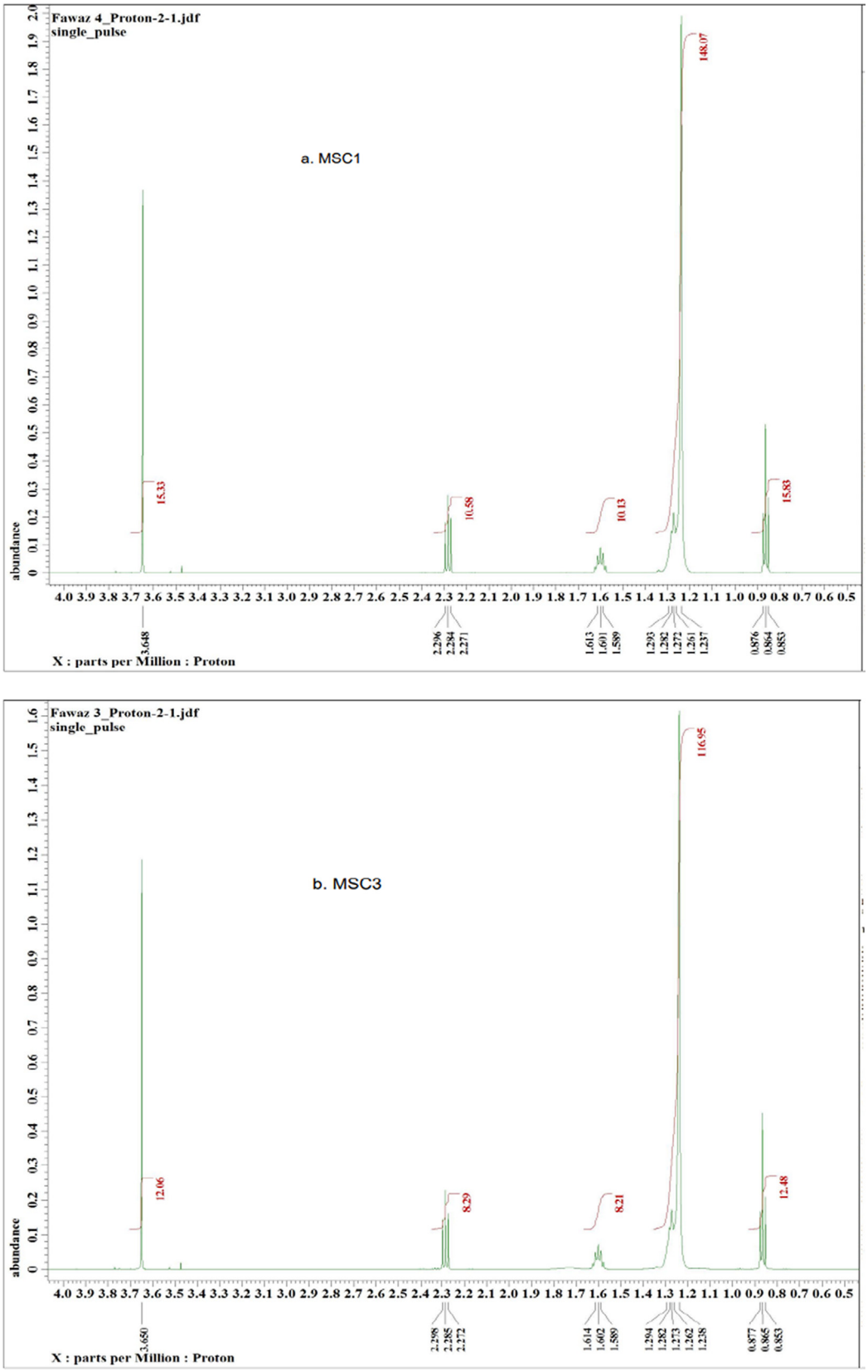

Fig. 2. A typical ^{1}H NMR spectrum of samples a) MSC1 (1 g catalyst) and b) MSC3 (3 g catalyst) at reaction conditions. temperature 90 °C, 3 h, molar ratio of methanol to stearic acid 175.4:1, volume = 26–27 mL.

25 mg of sample was placed in the sampling accessory and the empty accessory was used to obtain the background spectrum [35–37]. Each spectrum was calculated as the average of 32 scans and subjected to background subtraction with the total time required for spectral collection of 5 min. The peaks were adjusted and smoothed and baseline correction was performed using the

Table 3
Molecular moieties of methyl esters and their 1H NMR chemical shifts [13].

Signal	Moieties	Chemical shifts
A	Methyl ester $-CH_3$	3.50–3.70 ppm
B	$-CH_2$-adjacent to the carbonyl group	2.24–2.29 ppm
C	The aliphatic $-CH_2$-s. CH_2 group which is one group away from carbonyl group.	1.61–1.28 ppm
D	$-CH_2$ - in CH_2R. CH_2 groups between the end CH_3 group and the CH_2 group	1.23–1.29 ppm
E	End of chain aliphatic $-CH_3$	0.85–0.87 ppm

Table 4
Percentage Conversion of FAMEs by ATR-FTIR, ^{1}H NMR and GC-FID.

Effect of molar ratio methanol to stearic acid (MR), 90 °C, 3 g cat,3h.				
Samples		MR	[%] ATR-FTIR ± RSD	[%] GC-FID ± SD	[%] ^{1}H NMR
MSMR 175:1		175:1	88.38 ± 0.28	73.62 ± 0.057	95.22
MSMR 87.7:1		87.7:1	97.20 ± 0.49	88.5 ± 0.0539	100.31
MSMR 35:1		35:1	88.84 ± 0.28	95.35 ± 0.049	98.99
SMR 19.5:1		19.5:1	76.46 ± 0.50	91.88 ± 0.132	95.9
Effect of catalyst amount, MR = 175:1, 3 h, 90 °C					
Samples		Cat. g	[%] ATR-FTR ± RSD	[%] GC-FID ± SD	[%] ^{1}H NMR
Blank		0	48.87 ± 0.1	52.26 ± 0.064	48.68
MSC1		1	90.44 ± 0.72	89.19 ± 0.075	93.6
MSC1.5		1.5	84.48 ± 0.14	77.65 ± 0.078	90.74
MSC3		3	88.38 ± 0.28	80.9 ± 0.046	97.22
Effect of catalyst amount, MR = 175:1, 3 h, 65 °C					
Blank		0	-	5.75 ± 0.73	[%] ^{1}H NMR
MSC1		1	-	70.41 ± 0.024	-
MSC1.5		1.5	-	73.99 ± 0.043	-
MSC3		3	-	80.56 ± 0.035	-
Effect of reaction time, MR = 175:1, 3 cat., 90 °C					
Samples		Time, h	[%] ATR-FTIR ± RSD	[%] GC-FID ± SD	[%] ^{1}H NMR
MST1		1	79.89 ± 0.21	69.04 ± 0.0727	85.70
MST2		2	81.04 ± 0.06	80.09 ± 0.0713	89.66
MST3		3	88.38 ± 0.28	80.9 + 0.0462	97.22
MST5		5	87.69 ± 0.28	82.14 ± 0.0438	90.86
Effect of reaction temperature, constant MR = 87.7:1, 3 h 3 g cat					
Samples		Temp °C	[%] ATRFIRT ± SD	[%] GC-FID ± SD	[%] ^{1}H NMR
MS 35 °C		35	-	72.81 ± 0.041	-
MS 45 °C		45	-	75.75 ± 0.085	-
MS 55 °C		55	91.20 ± 0.81	82.67 ± 0.0123	-
MS 65 °C		65	89.29 ± 0.78	89.06 ± 0.037	-
MS 75 °C		75	89.30 ± 0.4	85.75 ± 0.098	-
MS 90 °C		90	97.20 ± 0.49	88.5 ± 0.0539	-
Recycling of catalyst; MR 87.7:1, 65 °C, 3 h, 3 g of catalyst.					
Sample		No. cycle	[%] ATRFIRT ± RSD	[%] GC-FID ± SD	
MSR 1		1	-	88.50 ± 0.0539	
MSR2		2	-	89.85 ± 0.064	
MSR3		3	-	88.57 ± 0.07	
MSR4		4	-	94.10 ± 0.0513	
MSR5		5	-	93.91 ± 0.108	
MSR6		6	-	92.47 ± 2.89	
MSR7		7	-	80.21 ± 0.057	
MSR8		8	-	80.63 ± 0.0614	
MSR9		9	-	71.40 ± 0.076	
MSR10		10	-	73.0 ± 0.083	
MSR11		11	-	71.68 ± 0.037	
MSR12		12	-	60.0 ± 0.065	
MSR13		13	-	57.32 ± 0.055	
Regenerated of catalyst& reused. MR 87.7:1, 65 °C, 3 h, 3 g of cat.					
sample		No. cycle		[%] GC-FID ± SD	
MSR 1		1	-	84.0 ± 0.03	
MSR2		2	-	84.7 ± 0.03	
MSR3		3	-	10.2 ± 0.02	
Test homogenous via heterogenous ca. MR 87.7:1, 2 h, 65 °C, HT = heterogenous, HM = homogenous					
sample		Cat. [g]	[%] ATRFIRT ± SD	[%] GC-FID ± SD	
MS-HT		3	-	76.55 ± 0.01	
MS-HM		0	-	1.44 ± 0.01	
Effect of fatty acid chain; 3 h, 3 g cat. Molar ratio of Methanol. OA = 87.06:1 & methanol. PA = 87.06:1.					
Sample		Temp °C	[%] MP ± SD	[%] MO, ±SD	
MP35°C,	MO35°C	35	76.45 ± 0.02	63.49 ± 0.10	
MP45°C,	MO45°C	45	84.91 ± 0.01	66.9 ± 0.04	
MP55°C,	MO55°C	55	91.97 ± 0.06	68.56 ± 0.09	
MP65°C,	MO65°C	65	86.75 ± 0.03	65.91 ± 0.02	
MP75°C,	MO75°C	75	82.68 ± 0.04	68.02 ± 0.11	

SA = Stearic Acid, MS = Methyl Stearate, OA = Oleic Acid, PA = Palmitic Acid, MO = Methyl Oleate, MP = Methyl Palmitate, SD is given for triplicate sampling in each analytical technique.

integration mode B. The absorbance intensity was measured as peak height taken from the baseline over the wavenumber range of 1799–1658 cm^{-1} [27]. Analyses of sample unknowns were repeated fivefold and the averaged peak heights used.

ATR-FTIR analysis was carried out in transmission mode for the amidoximated PAN ion-exchange fibres (PANF), fresh acidified PANF catalyst and deactivated PANF. Spectra were gathered using 160 scans with 4 cm^{-1} resolution. Each sample was measured in triplicate and the following spectrum handling was carried out: Baseline correction, spectrum scaling and smoothing (2 × 25 smoothing points) and a final baseline correction and scaling.

Results and discussion

Qualitative analysis of methyl stearate

The ^{1}H NMR spectra of the model compounds methyl stearate (MS) and stearic acid (SA) used in this work are shown in Fig. 1a and 1b. The ^{1}H NMR spectra for the esterification products MSC1 and MSC3 are shown in Fig. 2a and 2b. Table 3 summarizes the functional groups and their chemical shifts. The high intensity of signal (A) belongs to the hydrogens of the methoxy group of the ester - OCH_3 at 3.60 and 3.70 ppm [13,39] and is clearly present for the methyl ester model compound (Fig. 1b) and for the two esterification products (Fig. 2a and 2b). This signal increases with the extent of conversion of acid to ester and Fig. 1a shows that this signal (A at 3.60 and 3.70 ppm) is absent for the pure stearic acid.

The triplet signal (B) at 2.24–2.29 ppm corresponding to the CH_2 group adjacent to the carbonyl group in stearic acid (see Fig. 1a) occurs at a slightly higher chemical shift (δ) value than in methyl stearate. This is likely to be because the carboxylic group of stearic acid results in more de-shielding as compared to the ester group (Fig. 1b) [39].

The intensity of this methoxy hydrogen signal (A) was found to increase on replacing 1 g of protonated catalyst (MSC1) with 3 g of protonated catalyst (MSC3), whereas the intensity and overall area of the triplet peak (B) for the acid decreases which indicates a higher conversion of stearic acid to methyl stearate (see Fig. 2a and b) [39]. Table 4 gives the reaction conditions for the esterification of stearic acid.

ATR-FTIR spectra of the model compounds methyl stearate (MS) and stearic acid (SA) are shown in Fig. 3. The ATR-FTIR spectra for the esterification products MSC1, MSC1.5 and MSC3 are shown in Fig. 4 and the reaction conditions are given in Table 4. The infrared spectra demonstrated two main regions. The first region is the fingerprint region from 400 to 1500 cm^{-1}, with the peak at 1160–1170 cm^{-1} due to the C—O vibrations of the ester group. The second region above 1500 cm^{-1} is the diagnostic region and can be used to determine the functional groups in the sample. Here, the intensity of the peak at 1735–1750 cm^{-1} is used to evaluate and indicate the carbonyl group (C═O) of the ester, as it is thought to be more reliable than the peak in the fingerprint region at 1160–1170 cm^{-1}. Whilst it is possible to identify the functional group in the fingerprint region of the FT-IR spectrum it is difficult to perform accurate quantification due to the noisy background.

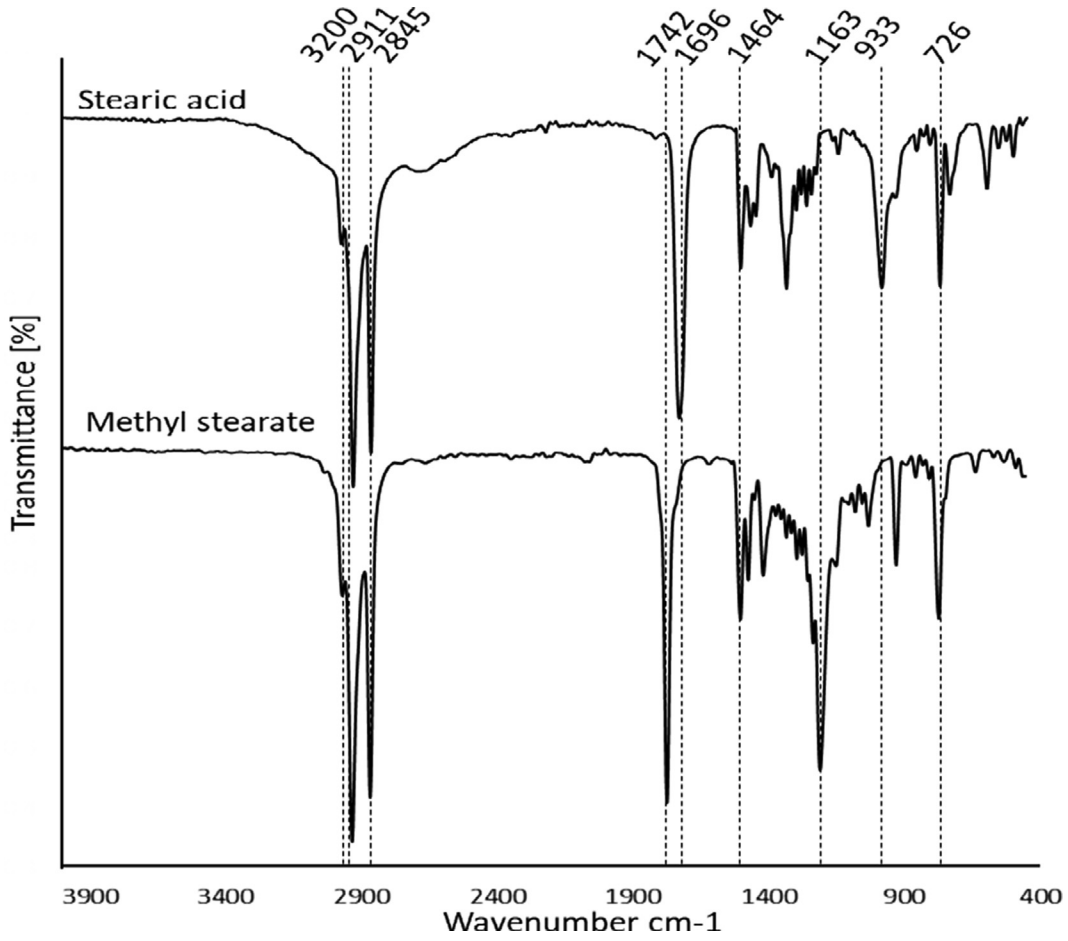

Fig. 3. ATR-FTIR spectra of a) stearic acid and b) methyl stearate.

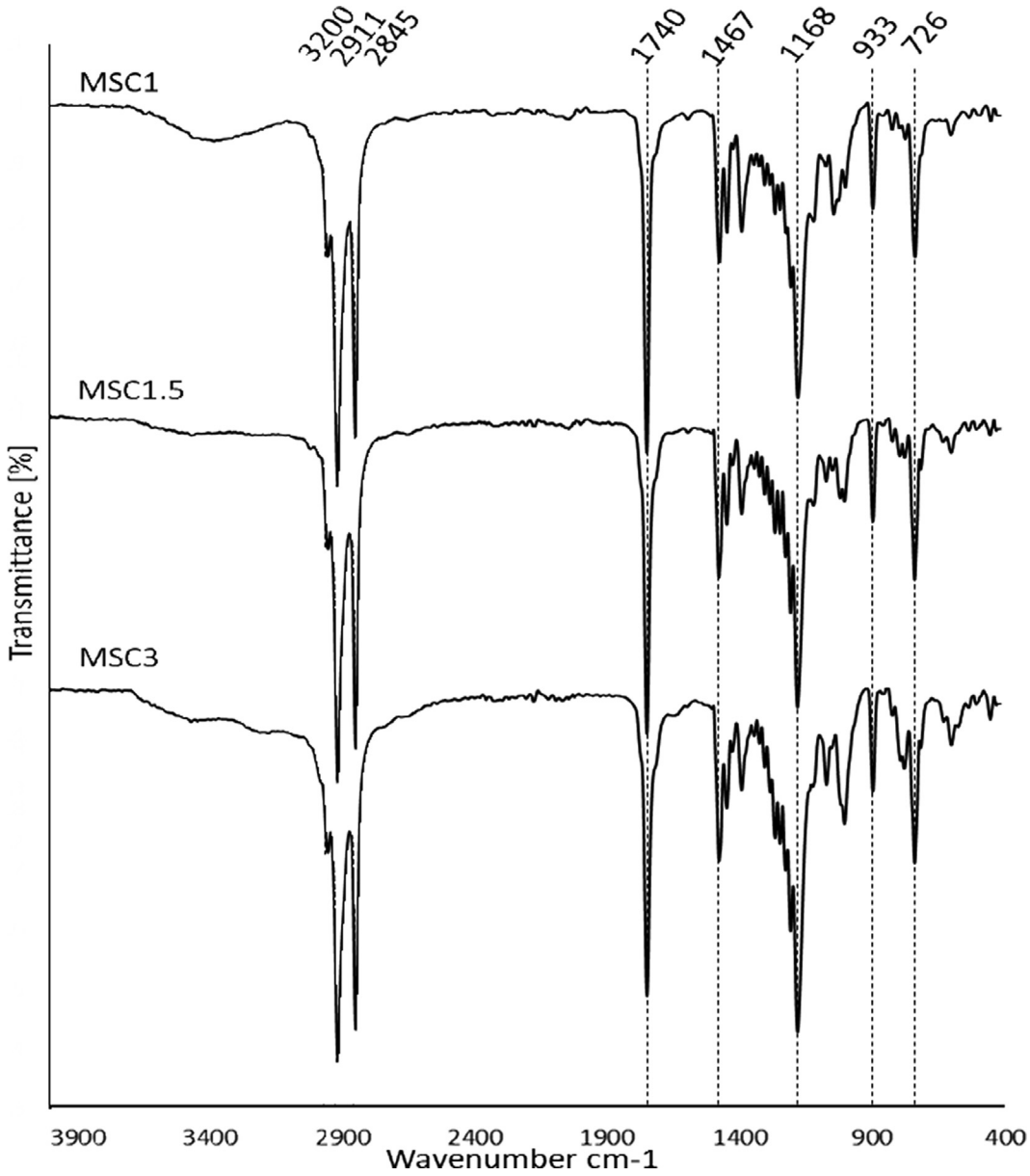

Fig. 4. ATR-FTIR spectra of products of esterification of stearic acid with methanol for on 1 g, 1.5 g and 3 g of protonated catalyst. a) MSC1 b) MSC1.5 and c) MSC3. Reaction temperature 90 °C, and 3 h, 175:1 molar ratio of methanol to stearic acid, volume = 26–27 mL.

The stearic acid (SA) spectrum (Fig. 3a) shows a broad peak from 3200 to 2500 cm^{-1}which can be assigned the O—H stretch in carboxylic acids [40]. This peak also overlaps with the asymmetric and symmetric stretching of the CH_2 groups centered on 2910 cm^{-1} and 2845 cm^{-1}, respectively [40]. The intense peak at 1696 cm^{-1}, can be assigned to the C═O in the carboxylic acid. The band at 1298 cm^{-1} results from a mixture of O—C—O and OH intensities within the COOH group [40]. The band at 933 cm^{-1} is assigned to of the O—H bond in dimeric stearic acid as a result of an angular deformation outside the plane [40]. The band at 726 cm^{-1} is representative of the combined rocking of all CH_2 groups in the aliphatic chain [40]. Finally, these bands in the IR spectrum indicate the presence of carboxylic acids [27,40,41,42].

Fig. 3b shows the IR spectrum of methyl stearate (MS). This figure displays many identical bands to that of stearic acid (SA), but there is some evidence of ester formation. The sharp and strong band attributed to the carbonyl stretching mode in the ester moved from 1691 cm^{-1} for stearic acid to 1735–1750 cm^{-1}. Also, a new sharp band centered at 1160–1170 cm^{-1} is characteristic of the C—O stretch in the ester [40]. These two bands indicate the presence of esters in the infrared spectra [27,40,41,42]. Absence of the peak at 1696 cm^{-1} in Fig. 4 for all products (See Table 4) of the esterification reaction is indicative of the absence of stearic acid indicating high conversion of stearic acid (SA) to methyl stearate (MS) in our reaction conditions. Fig. 4 shows the infrared spectra for those products produced on increasing the amounts of protonated catalyst from 1 g to 3 g (MSC1, MSC1.5 and MSC3), at reaction conditions: temperature 90 °C, 3 h reaction time, molar ratio of methanol to stearic acid of 175.4:1 and volume 26–27 mL. The peak intensities of the carbonyl group at 1741–1750 cm^{-1} and the C—O group at 1160–1166 cm^{-1} are similar in intensity regardless of the amount of catalyst used. The esterification of stearic acid (SA) and the formation of methyl stearate (MS) for all samples in this work were thus confirmed by both ^{1}H NMR and ATR-FTIR techniques.

Quantitative analysis of FAMEs

The esterification process, is limited by low conversion requiring long reaction times due to the establishment of equilibrium [10]. Ester hydrolysis, the reverse reaction to esterification, is initiated by the reaction product- water. To avoid the equilibrium establishment and to improve conversion, many studies have been conducted, however a substantial difference between current industrial practices and optimum esterification process/conditions persists until now [10]. In the following section, the reaction parameters are optimized to increase the ester product.

Effect of molar ratio of alcohol to acid

The effect of variation in the molar ratio of alcohol to acid on the esterification of stearic acid is given in Table 4 and shows that the highest percentage conversion of methyl stearate is 95.35 ± 4.09 % with regards to the duplicate experiments (See Table 4 for SD as regards triplicate sampling and Fig. 5 error bars for batch reproducibility on conversion %) and that conversions were over 69 % for all reaction parameters used. At a low methanol to acid molar ratio of 19.5:1, the conversion to methyl stearate was 91.88 % based on GC-FID analysis, which increased to 95.35 ± 4.09 % on increasing the methanol to acid molar ratio to 35:1, as excess methanol facilitates the esterification reaction in the forward direction. By further increasing the methanol to acid ratio to 175:1, the conversion of methyl stearate gradually decreased due to a dilution effect arising from the production of water covering the active sites of the protonated catalyst. This may hamper the acidic protonation at the active sites resulting in marginally lower activity. This phenomenon has been seen in a number of other studies. In Ezebor F. et. al. [43], protonated catalysts prepared from oil palm trunk (OPT) and sugarcane bagasse (SCB), were used to synthesize ethyl palmitate and butyl palmitate [3]. The optimum molar methanol to acid ratio was found to be 18:1, with an excess of methanol having a negative effect on catalytic activity [43]. Similar observations were reported by other studies [44–46], where FAME yield increased with increase in methanol: acid molar ratio, but was inhibited by any further increases.

Hence, the methanol to acid molar ratio of 35:1 was chosen as optimal. The conversion of stearic acid calculated from ATR-FTIR was found to differ considerably as compared with conversions obtained from GC-FID. This could be explained by a number of reasons, the first is that the GC-FID technique is more sensitive and accurate as compared to ATR-FTIR, which is considered to be a semi-quantitative analysis. The second reason is that the measurements for ATR-FTIR were taken using solid samples, which were ground into very fine particles. The physical grinding and mixing of the samples were found to be difficult, and the composition of the samples may not be homogenous. Another reason is that it is difficult to read the peak beginning and end positions on the base line.

Effect of the amount of protonated catalyst

In theory, the more protonated catalyst that is added the greater the rate of production and conversion to the products as confirmed by our results. The conversion to methyl stearate increases when the amount of protonated catalyst increases from 1 g to 3 g at 65 °C (See Table 4 and Fig. 6). This could be explained that by increasing the amount of protonated catalyst and thus acid sites, there is a higher probability of the reactants interacting with active sites and thus increasing the yield of ester [3].

This is also seen in other studies. For example, Zhang Q. et al. [32] reported the effect of the amount of catalyst (1–12 wt. %) on the conversion of lauric acid. The catalyst was a solid acid nano cat-

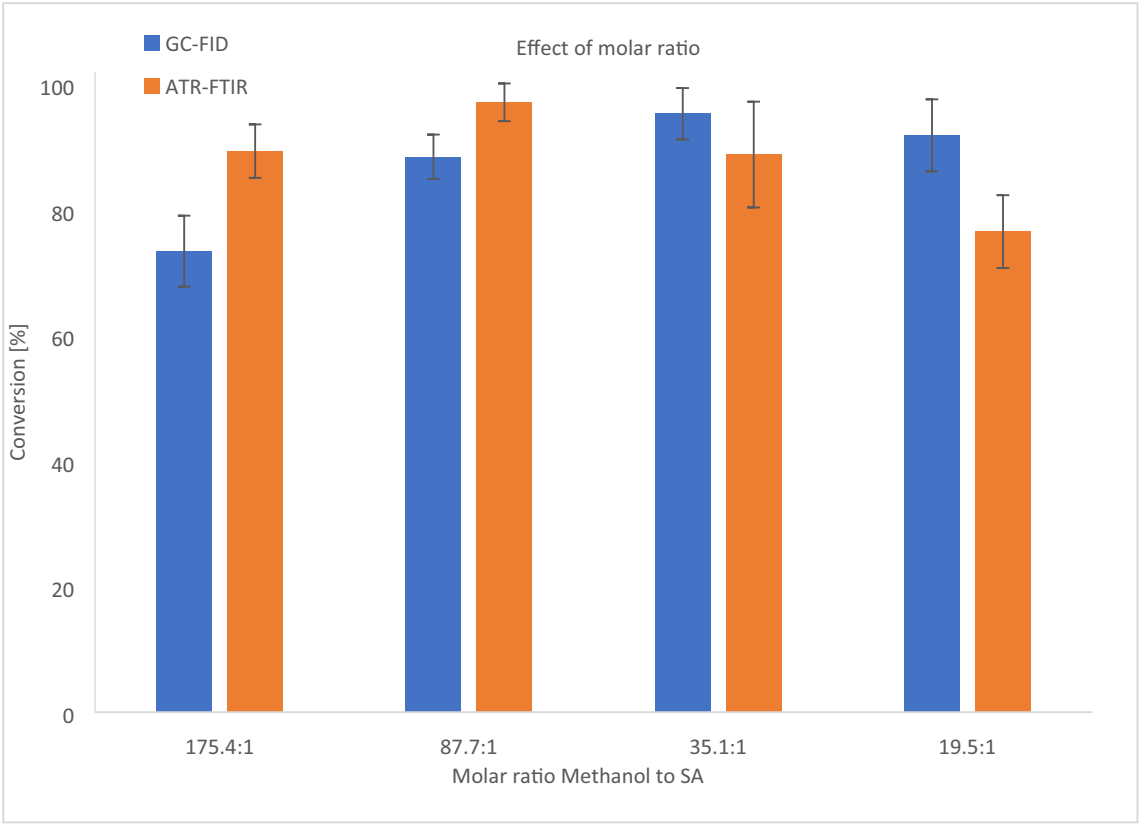

Fig. 5. GC-FID and ATR-FTIR analysis for the conversion of stearic acid to methyl stearate as a function of their molar ratio, a) MSMR- 175:1, b) MSMR- 87.7:1c) MSMR- 35:1 and d) MSMR −19.5:1; reaction conditions. temperature 90 °C, and 3 h, 3 g of protonated catalyst, volume 26–27 mL.

alyst (Ag_1 $(NH_4)_2PW_{12}O_{40}$/UiO-66) comprising of ammonium and silver co-doped $H_3PW_{12}O_{40}$ and a zirconium-based metal – organic framework (UiO-66) [32]. Neji [33] studied the effect of catalyst loading from 0.01–0.2 % w/w of commercial acid clays (KSF, KSF/0, KP10, and K10) on the conversion of stearic acid with ethanol, at 150 °C, for 4 hours and found also that conversion to the ester increased proportionally with the amount of catalyst [33]. Interestingly, above a catalyst concentration of 0.1 %w/w, the fatty acid conversion peaked at 97 % and did not increase further [33]. Fig. 6 shows that at the higher reaction temperature of 90 °C the extent of conversion is maximized at 1 g of protonated catalyst as shown by GC-FID which supports Neji that there is an optimum catalyst to acid ratio, although ATR-FTIR suggests that the extent of conversion is similar for 1,1.5 and 3 g of catalyst.

Effect of reaction time

The effect of reaction time on rate of conversion was studied for a molar ratio of alcohol: stearic acid of 175:1, at 90 °C, with 3 g of protonated catalyst. GC-FID analysis shows that over the first 1 hour to 2 hours of reaction, product conversion rose from 69 % up to 80 %, but afterwards increasing reaction time to 3 and 5 hours there was a negligible further increase in conversion from 80 % to 82 % (See Table 4 & Fig. 7).

Thus, equilibrium was achieved within 2 hours most likely because with the longer reaction time, the concentration of products gradually increases which slows down the forward reaction [47]. Additionally, other side reactions might occur with the increase in reaction time, decreasing the conversion of the esterification reaction [48,49]. Therefore, the optimum reaction time is 120 min as the equilibrium state is achieved under these conditions with no further increase in methyl stearate [MS].

Effect of reaction temperature

The conversion to the ester was positively correlated with reaction temperature. On increasing the reaction temperature up from 35 °C to 65 °C conversion increased from 72.81 % up to 89.06 % (See Table 4 & Fig. 8), after which the rate of conversion reaches a steady state. This increase in the reaction temperature further increases collisions between molecules, which in turn boosts the reaction rate [50]. Also, the forward reaction is endothermic and favoured by increasing temperature. There is no significant increase in the ester between 65 °C and 90 °C. [18,51,52], because as temperature increases there is potential for loss of methanol on refluxing in an open reaction vessel. It was also noticed that there was increasing darkening in the color of the product at higher temperatures (>80 °C). With increasing reaction temperature, there will ultimately be an increase in production costs in industry [51–53] therefore, in order to save energy, a reaction temperature of 65 °C was chosen as the optimum reaction temperature.

Protonated catalyst recycling and regeneration

To investigate the extent of re-use of the protonated catalyst in the esterification reaction the catalyst was removed and fresh feed was added to the reactor. The process parameters used were: 87.7:1 molar ratio of methanol to stearic acid, 65 °C, 3 h and 3 g of protonated catalyst and volume 26–27 mL. It was found that the protonated catalyst maintained high catalytic activity for the

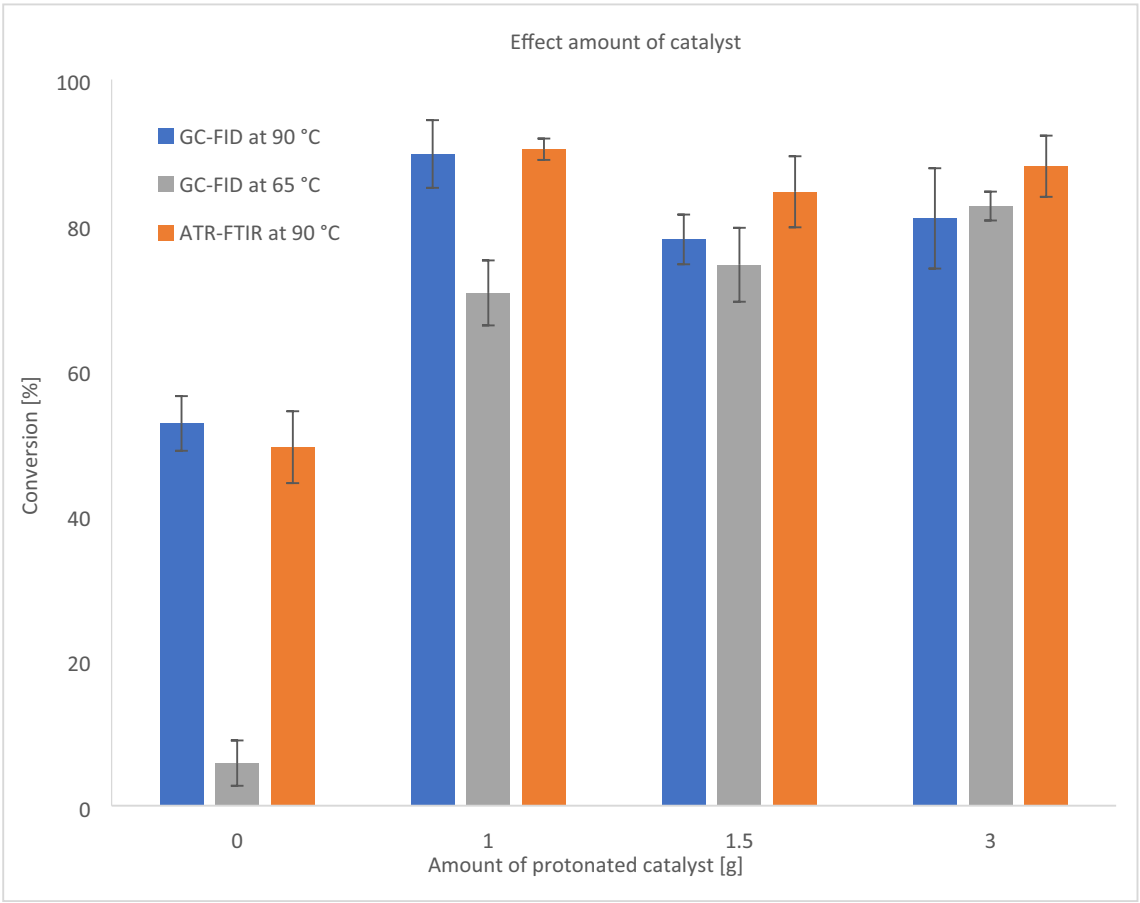

Fig. 6. GC-FID and ATR-FTIR analyses for conversion of stearic acid to methyl stearate as a function of the amount of protonated catalyst from 1 to 3 g, a) no protonated catalyst b) MSC1, c) MSC1.5, and d) MSC3, at reaction temperature 65 °C and 90 °C, molar ratio of methanol. acid of 175:1, 3 h, volume 26–27 mL.

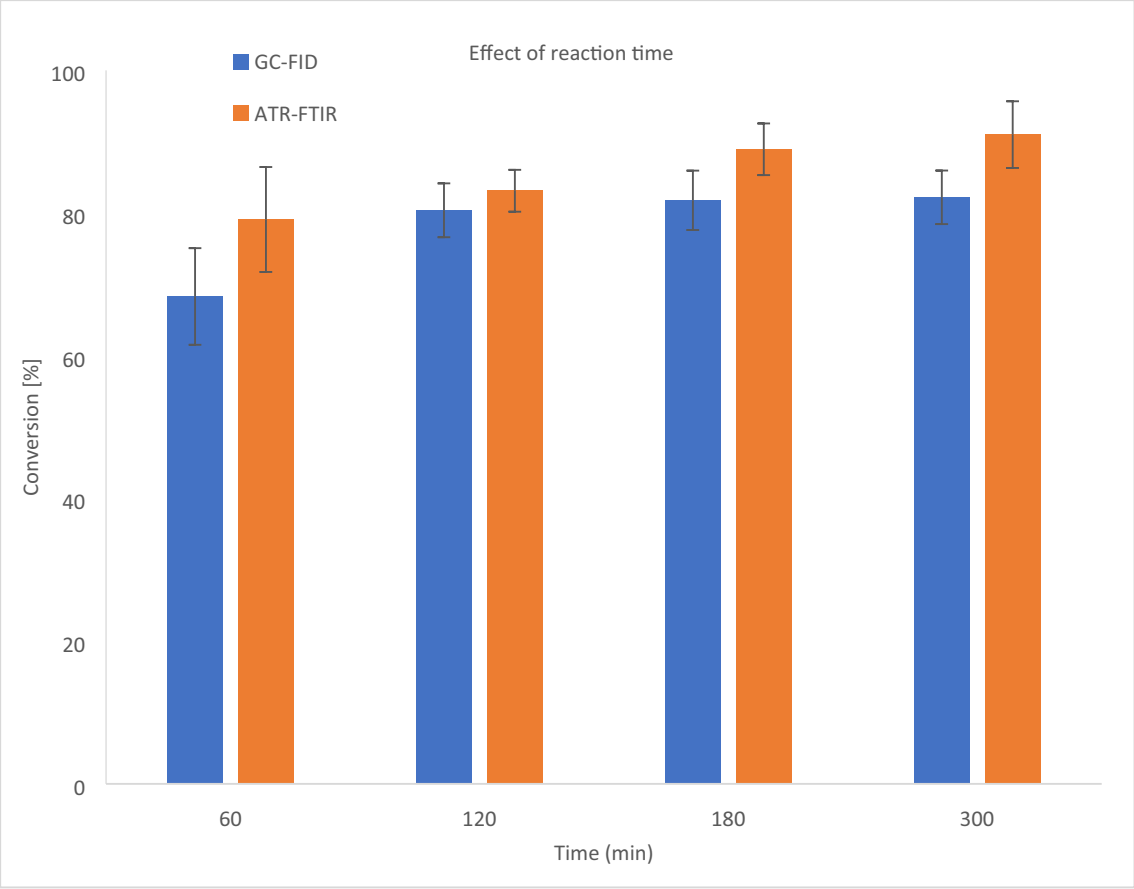

Fig. 7. GC-FID and ATR-FTIR analyses for conversion of stearic acid to methyl stearate as a function of time, for 1, 2, 3 and 5hours a) MST1 b) MST2 c) MST3 and d) MST5, temperature 90 °C, and 3 h, with molar ratio of methanol to stearic acid of 175:1, 3 g catalyst, volume 26–27 mL.

first 6 cycles with conversion to the ester ranging from 90-94 %. This decreased to 80 % for the seventh and eight cycles of use, showing good stability of the protonated catalyst (See Table 4 and Fig. 9). The catalytic activity dropped to 57 % after 13 esterification cycles after which the catalyst was regenerated.

To investigate regeneration of the protonated catalyst for repeated use, the protonated catalyst was recovered after the 13th cycle of reaction and washed briefly with dimethyl chloride (DCM) to dissolve off any adsorbed organic reaction product. The protonated catalyst was regenerated with 30 ml of 2 M H_2SO_4 solution for 24hr and then dried for 24 h. Subsequently, the regenerated PANF acid protonated catalyst was reused in the esterification process. The catalytic activity of the regenerated PANF protonated catalyst was significantly regained to give 84 % conversion to methyl stearate for two more cycles (see Fig. 9 &Table 4). However catalytic activity sharply decreased after the second cycle with conversion reduced to about 10 % for the third cycle.

Deactivation of heterogeneous acid protonated catalysts can be via three mechanisms: the adsorption and subsequent blockage of active sites by reaction products, the leaching and loss of catalytic active sites into solution and the structural degradation of the catalyst [54,55]. Thus, one of the possible reasons for the drop in the catalytic activity was due to leaching of the protons/hydrogen sulphate ion/sulphuric acid from the PANF protonated catalyst. It could also be due to blocking of the acid sites of the catalyst. On regeneration after the 13th cycle of use, conversion to the ester was similar to that of the original experiments, but then dropped significantly. It is likely that the quick wash at ambient temperature was not sufficient to desorb any unreacted stearic acid or methyl ester from the protonated catalyst surface as will be shown in section 3.5 below. It is also possible that both the stearic acid and the methyl ester prevented the sulphuric acid from protonating the amidoxime functionalised PANF solid catalyst. The recovery of catalytic activity of the protonated catalyst after regeneration was then due solely to sulphuric acid absorbed between the fibrils of the fibrous catalyst, which exhaustively leached out after the second cycle resulting in its poor performance on the third cycle after regeneration. However, a more extensive regeneration protocol of the protonated catalyst of our work needs to be investigated to see if efficacy after regeneration can be improved. None the less, our heterogenous acidified PAN fibrous solid protonated catalyst showed a very high catalytic activity after thirteen cycles and also for two cycles after regeneration as compared to other works [50,55,56,57]. For example, sulphonated incompletely carbonized coffee beans [55] had conversions of between 40–60 % on first use which reduced to 10–20 % on 5th re-use in the esterification of caprylic acid. Esterification of waste cooking oil using a sulfonated montmorillonite clay acid catalyst [50] obtained 80.8 % conversion in the first cycle which was reduced to 60 % and 52 % in the second and third cycles, respectively [50]. Amberlyst-15 a sulphonated catalyst studied by Zhang et al (2020), demonstrated poor catalytic reusability, with a decrease in catalytic activity from 67.6 % in the 1st cycle to only 28.4 % in the 6th cycle [57]. Incorporating sulphonated resin in polyvinyl alcohol gave 98 % conversion with activity decreasing only slightly to 87.2 % after six runs [57] with reaction conditions: acidified oil 20 g; stirring rate 360 rpm; methanol:acidified oil mass ratio 2.5: 1; catalyst dosage 5 g; tem-

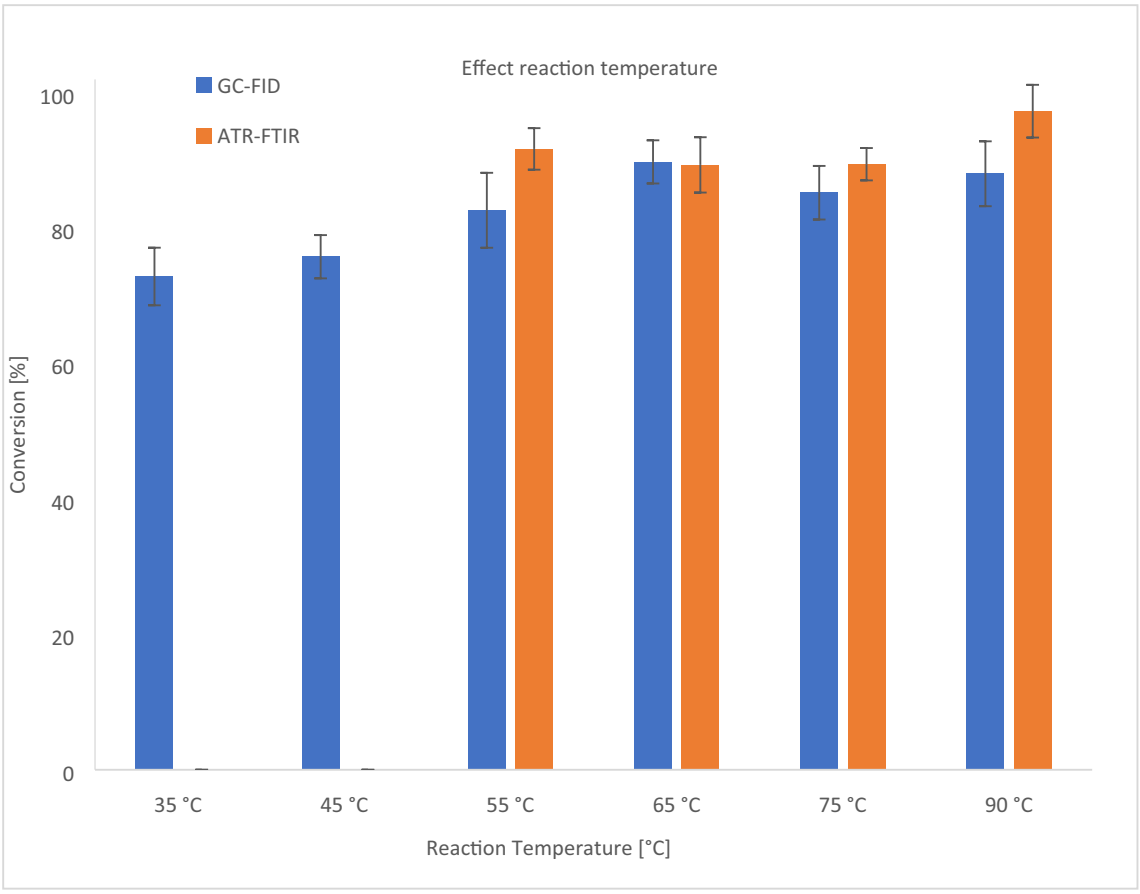

Fig. 8. GC-FID and ATR-FTIR analyses for conversion of stearic acid to methyl stearate as a function of temperature a) MS 35 °C, b) MS 45 °C c) MS 55 °C and d) MS 65 °C, e) MS 65 °C, f) MS 75 °C and h) MS 90 °C; reaction condition. (3) h, 3 g of protonated catalyst, molar ratio of methanol to SA was 87.7:1, volume 26–27 mL.

perature 65 °C. The re-usability of Amberlyst 45 was studied by multiple recycling experiments by Cabral et al. [58] in transesterification/esterification with reaction conditions of 1:18 oil: ethanol, 10 wt. % of catalyst loading, 120 min and 170 °C. Amberlyst 45 proved to be active after five cycles of use (yield of FAEE was 70.9 %) with no decrease in yield [58]. Whilst some of these comparisons were performed on waste oils and our work here was on model compounds the PANF acid mesh catalyst shows promise for the industrial treatment of waste oils as it has been recycled for longer and at considerably lower reaction temperatures as well as using lower reaction times. Reusability of the catalyst is important for commercial use at industrial scale.

Recently Ghorbani-Choghamarani A. et al., in 2022 described an efficient biodiesel production from oleic and palmitic acids using novel molybdenum metal–organic frameworks (MOFs) [59]. The catalyst showed almost constant efficacy of 92 % over 4 cycles in the esterification of oleic acid at reaction conditions of oil: methanol molar ratio of 1:13 and MOF (300 mg) at 60 °C for 4 h [59]. The main disadvantage of this catalyst as compared to our acid PANF mesh catalyst is the longer reaction time, the complexity of catalyst synthesis, the pressure drops experienced on using powdered catalysts and difficulties in the separation of the powdered catalyst at the end of esterification process which adds further cost.

ATR-FTIR analysis of the acidified protonated catalyst

Fi***gure 10 (3900–400 cm^{-1}) and the expanded (2,000–400 cm^{-1}) Fig. 11 shows the ATR-FTIR spectra of PANF ion exchange fibres, sulphuric acid protonated PANF catalytic fibres, re-basified fibres and deactivated fibres, whilst Scheme 3 shows their structures. The assignments can be seen in Table 5. Amidoximated PANF ion exchange fibres show a broad band in the 3300 – 3100 cm^{-1} regions assigned to a mixture of Nh, NH_2 and O—H bonds from amidoxime and amidrazone groups. The intense band at 1626 cm^{-1} and 1590 cm^{-1} is assigned to both C═N, NH_2 and C═O moieties. The amidoxime N-OH peak is also present at 920 cm^{-1}.

On acidification, the 3300 cm^{-1} peak reduces in intensity due to the protonation of NH and NH_2 groups to NH_2^+ and NH_3^+, this is also the case for the 1512 $cm^{-1}NH_2$ peak. The amidoxime N-OH peak at 920 cm^{-1} is possibly shifted to the shoulder at 965 cm^{-1} due to protonation. The C═N peak at 1626 cm^{-1} decreases in intensity on acidification which suggests acid hydrolysis of the amidoxime group (C = NOH) to amide (C═O) via Beckmann rearrangement. This also leads to the production of the intense C═O amide peak at 1678 cm^{-1}. There are also intense sulphate peaks at 1143, 1015, 860 and 570 cm^{-1} on acidification with the sulphuric acid. These sulphate groups are likely to be held electrostatically to the protonated NOH, NH and NH_2 groups of amidoxime and the protonated NH and NH_2 groups of any amidrazone groups present. The acidified fibres act as the protonated catalyst. Upon re-basifying the protonated catalyst to see if protonation is reversible, the intense sulphate peaks disappeared and the 910 cm^{-1}N-O amidoxime peak was once again visible, albeit weak in intensity. The NH_2 peak at ~ 1512 cm^{-1} was also reformed into an intense peak as well as the NH and NH_2 peaks in the 3300 cm^{-1} regions. This confirms that the acidified catalyst is formed by protonation of the NH, NH_2 and NOH groups by the sulphuric acid. The C═N peak at 1626 cm^{-1} peak does not return to its original intensity, signifying conversion of oxime to amide.

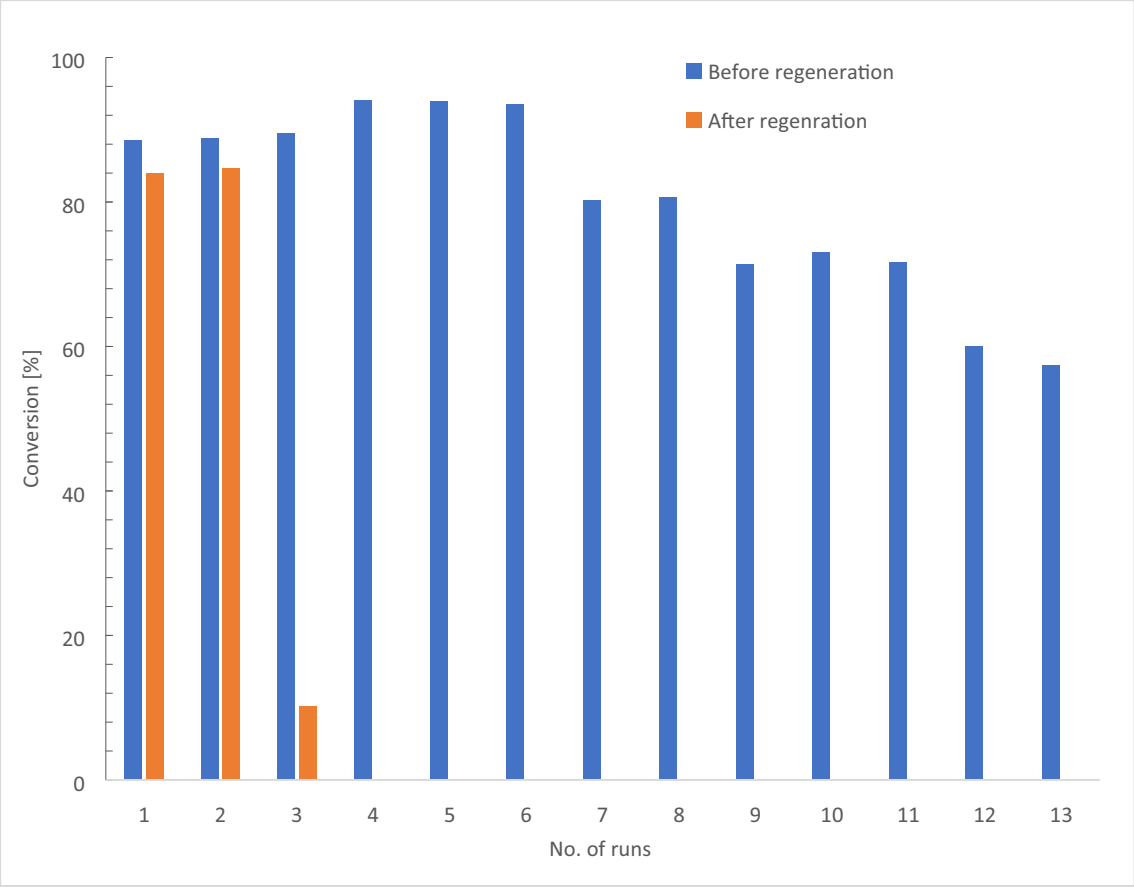

Fig. 9. GC-FID analysis for conversion of stearic acid to methyl stearate as a function of number of cycles. Reaction conditions. 65 °C, 3 h, 3 g of protonated catalyst, molar ratio methanol to SA was 87.7:1, volume 26–27 mL.

Table 5
FTIR assignments of the PANF ion exchange fibres, acidified and deactivated fibres. [24 60 61].

Wavenumber cm^{-1}	Ion exchange PANF	Acidified	Deactivated	Assignment
3300	X	X		NH_2/NH, amidoxime, amidrazone and amide on acidification
3165	X	X		OH, amidoxime
2976	X	X	X	C—H
2850	X	X	X	C—H
1741			X	C═O, ester
1678		X	X	C═O amide
1626	X	X	X	C═N, amidoxime
1512	X	X		NH_2, amidoxime and amide on acidification
1450	X	X	X	CH_2
1380	X	X	X	C—N
1250	X		X	C—O
1143		X	X	SO_4^{2-}
1015		X		SO_4^{2-}
920	X			N-OH, Amidoxime
860	X	X		SO_4^{2-}
570			X	SO_4^{2-}

After regenerating the sample that had been used for 13 cycles with a dichloromethane (DCM) wash and following sulphuric acid acidification, there was an initial increase in esterification activity with 84–85 % conversion. However, the activity on the third cycle dropped significantly to 10.16 %.

The ATR-FTIR spectrum of the deactivated catalyst can shed some light on what has happened to the structure of the catalyst on deactivation. Fig. 10 and the expanded spectrum of Fig. 11 shows the absence of the strong SO_4^{2-} peaks at 1143, 1015, 860 and 570 cm^{-1} which were seen in the acidified samples. Instead, there is a strong C═O peak from the methyl stearate ester at 1741 cm^{-1}, as well as, peaks arising from C—H groups at 2976 and 2850 cm^{-1}. This is likely to be due to the sorption and poisoning of the protonated catalyst by methyl stearate. The NH_2 groups (~3300 cm^{-1}) in the PAN acidified catalyst are almost completely removed or masked (ATR-FT-IR is a surface sensitive technique) as

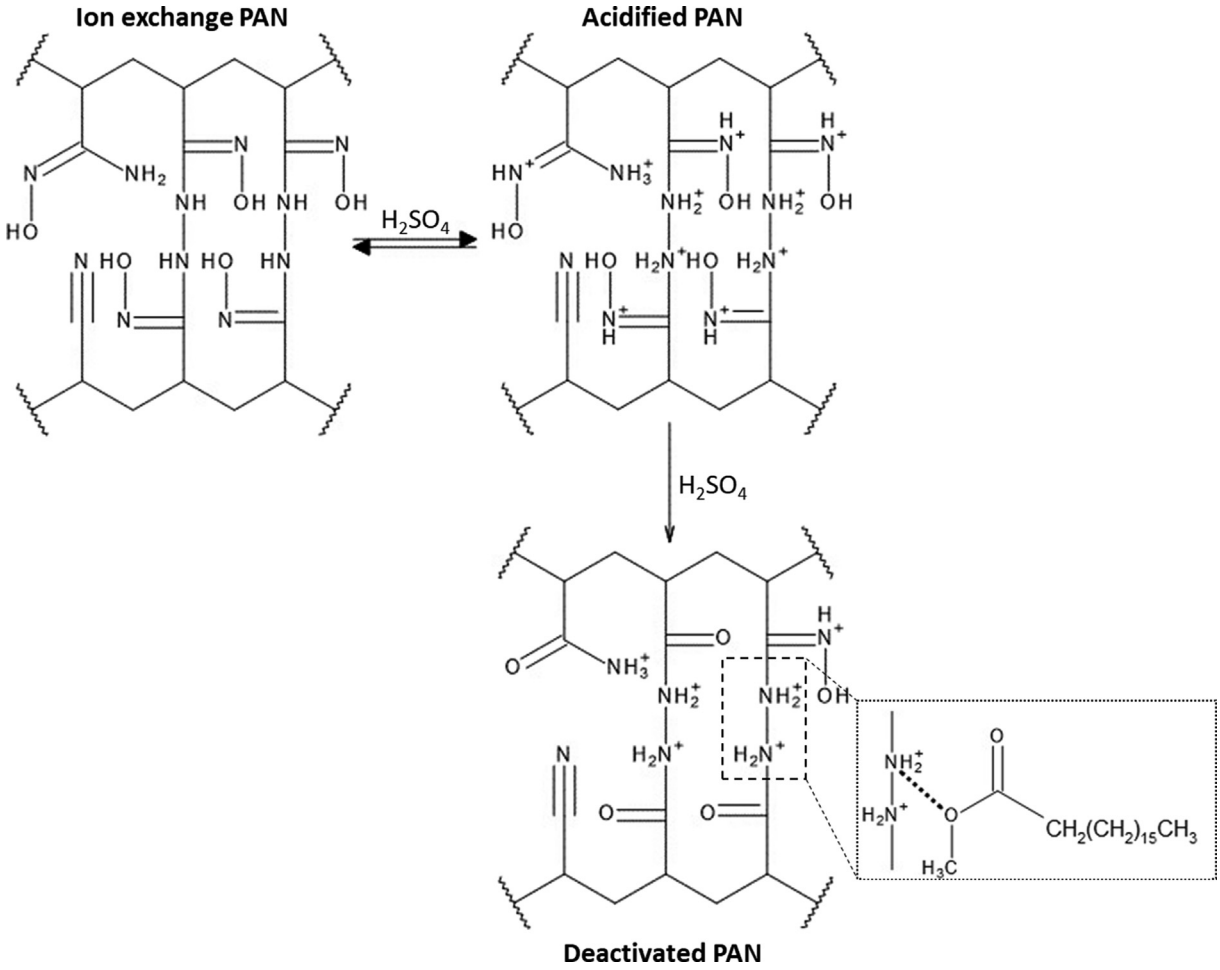

Scheme 3. Scheme showing the simplified structures of (i) ion exchange PAN, (ii) PAN acidified by protonation with sulphuric acid and (iii) deactivated PAN with amidoxime conversion to amide and the blocking of the acid sites by methyl stearate (MS).

is the NH_2 peak of the amidoxime, amidrazone groups and amide groups at 1512 cm^{-1} in the deactivated sample. However, the N-OH groups are still present as a shoulder at 965 cm-1 (Fig. 11) which suggests that there are still some acidified oxime groups present. The oxime group, via amide conversion, is likely to have been converted to a carbonyl group (amidoxime goes to amide type functionality) as shown by the strong C=O peak at 1678 cm^{-1} which is not unexpected owing to the repeated acidic heating of the protonated catalyst in the esterification reaction. The pKa of amide moieties is very low and similar to the pH of 2 M sulphuric acid suggesting it is less likely to be protonated in contrast to the amidoxime moiety which has a high pKa. Thus, it is likely that the acid treatment and prolonged heating during esterification resulted in a loss of functional groups that could be easily protonated and which was exacerbated owing to masking and blocking by the adsorbed methyl stearate.

Fig. 12 compares the ATR-FTIR spectra of the deactivated catalyst with both methyl stearate and stearic acid. It can be seen that the presence of the strong peaks at 1741 cm^{-1} and 1143 cm^{-1} on the deactivated catalyst are indicative of methyl stearate. Thus, the ATR-FT-IR supports the observed results in that the brief wash with DCM before regeneration did not remove adsorbed methyl stearate and the sites for protonation were blocked. The two cycles after regeneration led to high conversion to methyl stearate (most probably due to the leaching of sulphuric acid trapped between the fibrils) and which is likely to have lead to further blocking of the sites hastening deactivation.

Homogenous versus heterogenous catalytic activity

To explore whether the catalytic reaction is occurring in the heterogeneous or homogeneous phase the protonated catalyst is removed after reaction and the feed replenished. Two batches were set up with the same reaction conditions: 2-hours reaction at 65 °C, with a molar ratio of alcohol to acid of 87.7:1 and 3 g of protonated catalyst, volume 25 mL. After reaction one batch was analyzed by GC-FID to give 76.55 % conversion to methyl stearate (See Table 4 and Fig. 13). In the other batch the 3 g of protonated catalyst was removed after the esterification reaction and another 25 ml of methanol and 2 g stearic acid in the molar ratio of 87.7:1 was added and the reaction rerun for 2 hours at 65 °C. GC-FID analysis showed the conversion to methyl stearate was almost similar at around 77.99 %, showing that the added stearic acid only produced an additional 1.44 % conversion to methyl stearate. This showed that the second stage of reaction after taking out the protonated catalyst and rerunning the reaction with the same conditions, gave negligible conversion of product. This suggests that the reaction does not take place in the homogenous phase, but instead takes place on the protonated catalyst. This is why the acidified PANF solid protonated catalyst can be successfully recycled for 8 cycles

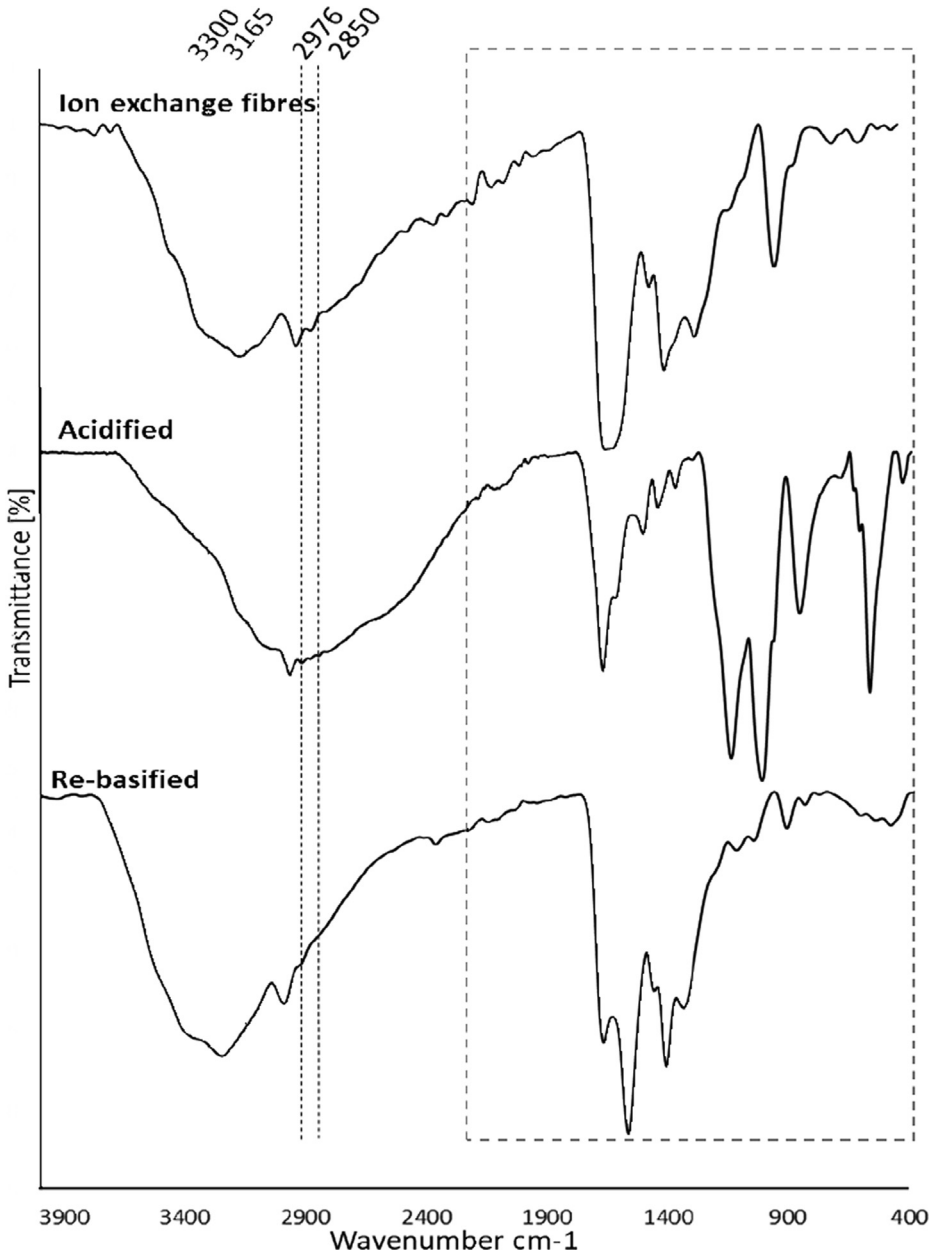

Fig. 10. Stacked ATR-FTIR spectra of the amidoximated PAN ion exchange fibers, and acidified catalyst. Re-basified spectrum is included for comparison with the protonated acidified catalyst. The area highlighted by the rectangle is expanded in Fig. 11. Assignments can be found in Table 5.

with 80 % conversion and up to 13 cycles with almost 60 % conversion.

Effect of fatty acid structure

Fig. 14 shows the influence of the C-atom chain length in saturated fatty acids and the presence of double bonds on conversion in the esterification reaction. Esterification reactions of stearic acid (SA) palmitic acid (PA) and oleic acid (OA) with methanol in presence of 3 g protonated catalyst over the temperature range of 35 °C to 75 °C were examined. The mole ratio of alcohol to SA, alcohol to PA and alcohol to OA were 87.7:1, 87.03:1 and 87.06:1, respectively. The results obtained showed that palmitic acid (PA) gave the highest conversion to methyl palmitate (MP) of 92 %. Double bonds in unsaturated fatty acids tend to result in a reduction in ester production [62–64] and thus it is unsurprising that oleic acid (OA) gave the lowest conversion of 68 %. This is thought to be because of the acid catalyzed addition of methanol to the C=C double bond to partially form the methoxylated oleic acid, which could then go on to produce the methoxylated methyl oleate (MO). The reaction of carboxylic acids in esterification reactions are also affected by steric factors in a linear alkyl series. In the work of Liu et al. [62] it was found that, from acetic to butanoic acids, the reaction rate declines with an increase in the length of carbon the chains. For higher acids only a minor effect on the reaction rate was observed with further increase in the number of carbon atoms. The longer the carbon chain is, the more difficult it is to react [64–67] and thus it is unsurprising that stearic acid (C18) gave a slightly lower conversion of 89 % than palmitic acid (C16) which had a conversion of 94 %.

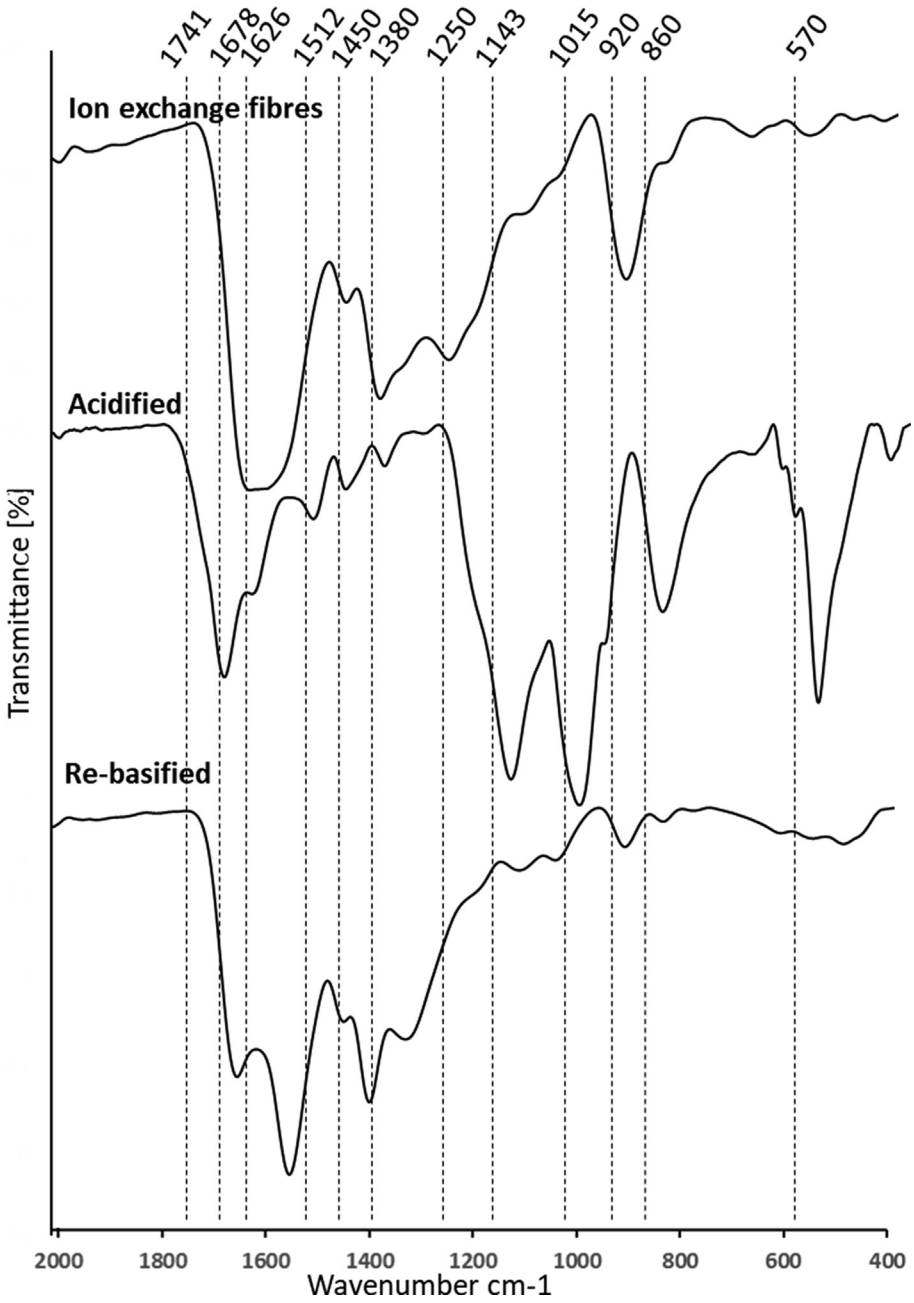

Fig. 11. Expanded 2000–400 cm^{-1} region of ATR-FTIR spectra of Fig. 10. Re-basified spectrum is included for comparison with the protonated acidified catalyst. Assignments can be found in Table 5.

Esterification mechanism

Strong acid sulphonated polymer catalysts such as Amberlyst-15 (sulphonated styrene–divinylbenzene cross linked polymer) are the most widely investigated acid catalysts used in esterification reactions, although more studies are looking into potential alternatives. Our amidoxime PAN fibres are weak base ion-exchangers containing a number of amine, crosslinked hydrazine and oxime groups capable of protonation by strong acids, such as, in this case sulfuric acid. Traditionally sulphonic acid groups which are bound chemically to a polymer to produce protonated catalyst surfaces begin the esterification process by donating a proton to the stearic acid molecule [3]. In the case of our PANF protonated catalyst the protons could potentially come from (i) protonated functional groups on the catalysts, such as, the amine, crosslinked amidrazone and oxime groups (as shown in scheme 3) or (ii) the proton from the monobasic species HSO_4^- arising from the partially dissociated sulphuric acid which is held electrostatically as a counterbalancing anion to the protonated groups of the catalyst. A similar mechanism for the uptake of sulphuric acid onto kaolinite in the presence of ammonia has been proposed by Zhang [68,3] using a mixture of theoretical and experimental methods. Focusing on proton transfer from the monobasic sulphuric acid to the carbonyl group of the stearic acid, the stearic acid undergoes a nucleophilic attack by the hydroxyl group of the methanol (CH_3-OH), and the reaction continues with water elimination followed by rearrangement to form the ester. The proton donating step is rapid, the nucleophilic substitution is known to be slow, whilst the reaction steps after the nucleophilic substitution are considered to be rapid. Finally, the surface of the protonated catalyst is

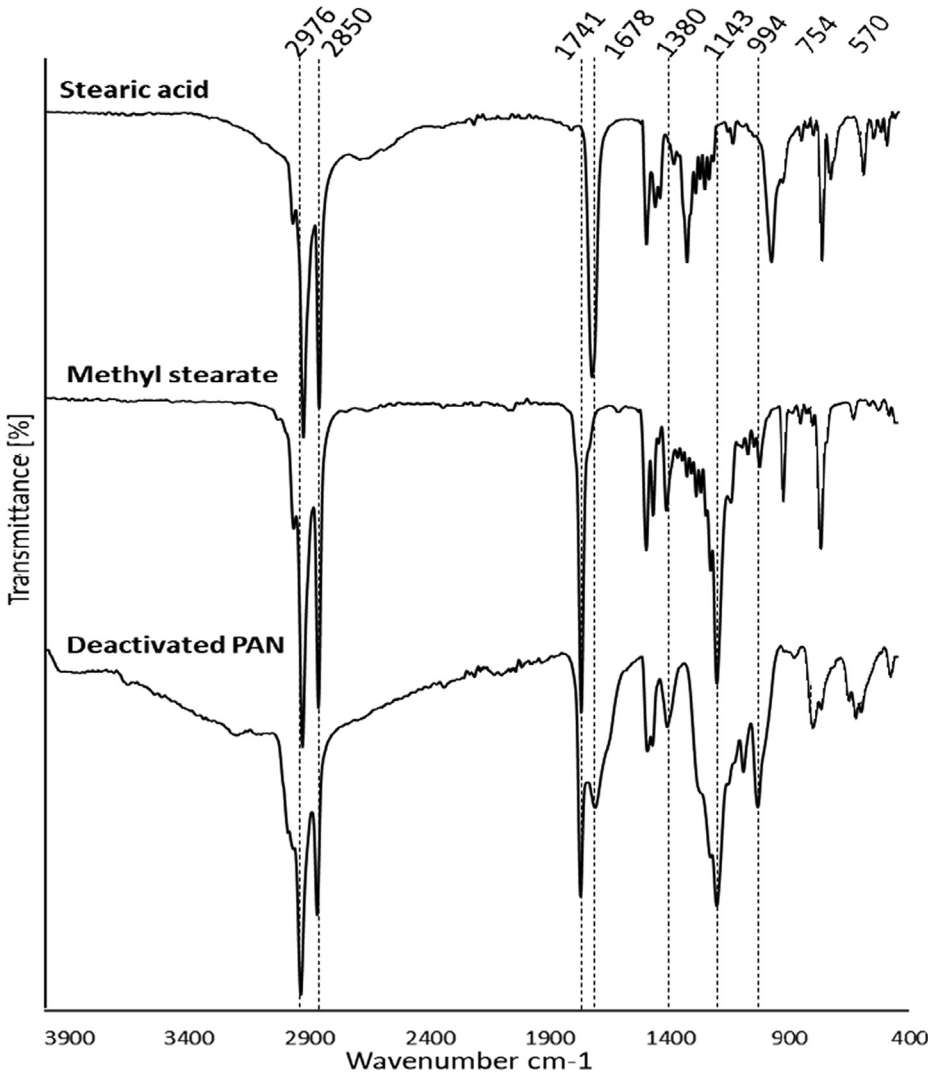

Fig. 12. Stacked ATR-FTIR spectra of the deactivated PAN with stearic acid and methyl stearate reference spectra.

free to participate in the next catalytic cycle. Others authors proposed a similar mechanism for the solid phase catalytic action [69–71].

The concentration of hydrogen ions on the external/internal surface of a solid acid protonated catalyst is much higher than that in the reaction medium [72] which potentially allows both better selectivity as well as reusability compared to homogenous catalysts. The potential for easy recovery and reuse as well as high yield of biodiesel suggest that heterogenous acid catalysts are potentially useful for biodiesel production [3].

Kinetic study

The kinetic profile of the esterification of stearic acid to give methyl stearate is given in Fig. 15. A set of experiments was carried out under the following conditions: 6 g of protonated catalyst, 87.7:1 methanol:stearic acid molar ratio with total volume 109.52 ml. The kinetic study was performed at temperatures of 45, 55, 65, and 75 °C and a sample was collected from the reaction vessel at pre-determined times. The methyl stearate conversion of each sample was determined by GC-FID. Fig. 15 shows that under these conditions the concentration of methyl stearate (MS) increased up to 60 min after which conversion slowed and started to approach saturation. The esterification reaction of stearic acid with methanol has a reaction rate that can be described by the Eq. (2).

$$-r_{0A} = k_1 C_{0A}^{\alpha} - k_2 C_{FAME}^{\beta} C_{water}^{\gamma} \quad (2)$$

Where, $-r_{0A}$ is the rate of reaction, k_1 & k_2 are the kinetic constants/ for forward/backward reactions, C_{0A}^{α} is the initial concentration of reactants, C_{FAME}^{β} is the concentration of FAMEs product, C_{water}^{γ} is concentration of water produced in the reaction and α, β and γ are the orders of reaction.

This equation will be applied with the following assumptions as suggested in [27].

(i) Throughout the reaction, the concentration of methanol can be considered as constant if it is in excess [27]
(ii) The excess of methanol results in the equilibrium significantly shifted towards the formation of products. Thus, the reverse reaction can be ignored [27,49].

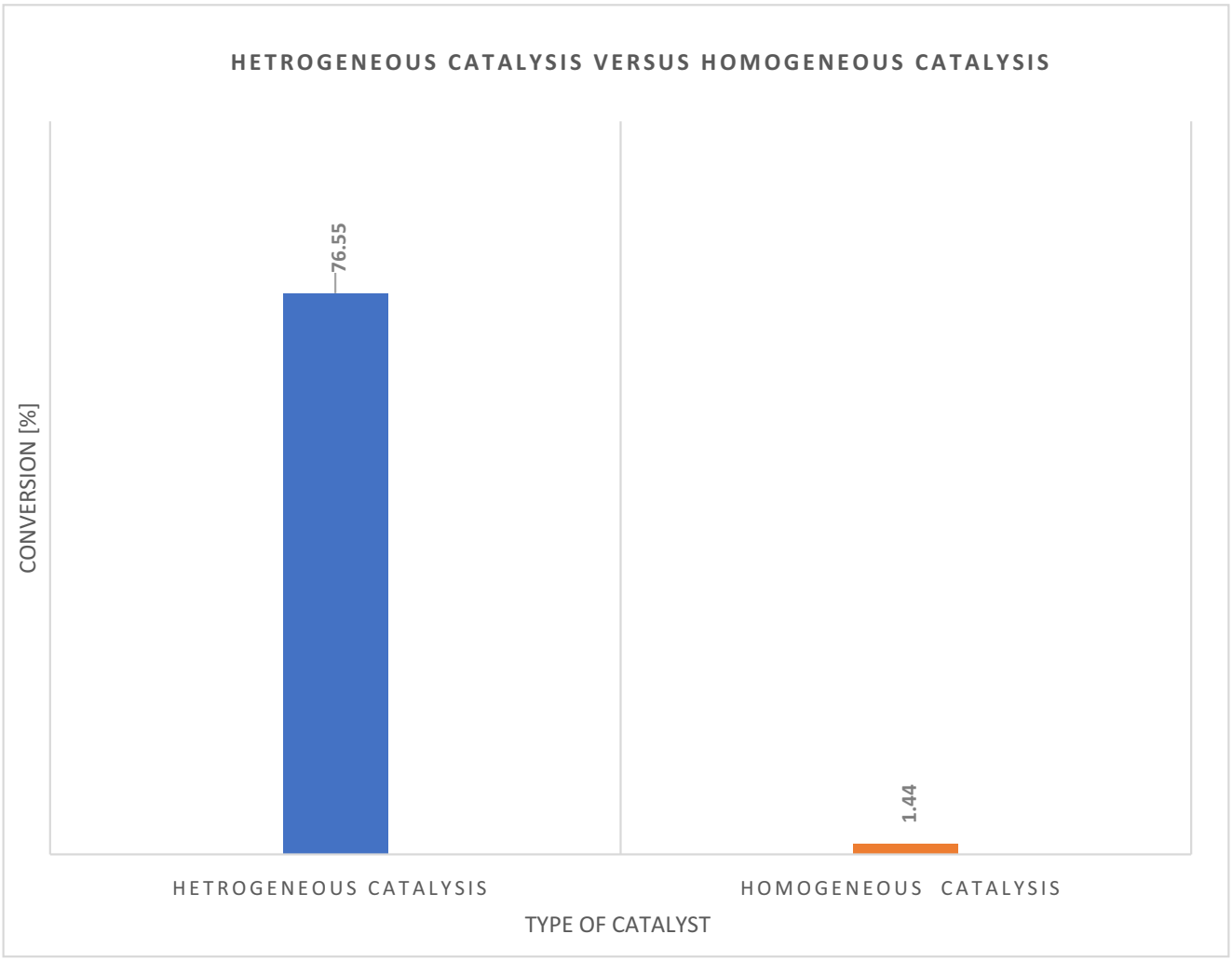

Fig. 13. GC-FID analysis for conversion of stearic acid to methyl stearate (i) in the heterogeneous phase with protonated catalyst and (ii) in the homogeneous phase after removal of protonated catalyst and replenishment of feed. Reaction condition. 65 °C, 2 h, 3 g of protonated catalyst, Molar ratio methanol to SA was 87.7:1. (heterogeneous); 0 g protonated catalyst (homogeneous).

The reaction rate then follows pseudo first order kinetics (equation (3)) as esterification becomes independent of the alcohol concentration [49]. The order of the reaction was determined by the integral method [23,40].

$$-Ln(1-X) = kt \quad (3)$$

where X is the stearic acid conversion at time 't' and k is the rate constant for the reaction.

The plot of -Ln (1- X) vs time is shown in Fig. 16 for the protonated catalyst at different reaction temperatures from 45 to 75 °C. The fitting results, correlation coefficient R^2, and the pseudo first-order rate (PFO) constants (k) are given in Table 6 where it is clear that the esterification data is a good fit to the PFO kinetic model (R^2) > 0.98 up to 0.99). The reaction rate constants (k) of these plots as listed in Table 6 were found to be 0.0094 min^{-1}, 0.0183 min^{-1}, 0.0186 min^{-1} and 0.0174 min^{-1} at 45, 55, 65 and 75° C, respectively. It suggests that apart from the reaction performed at 45 °C they have the same or very similar rates of reaction and that 55 °C is good enough (see Figs. 15 and 16). It is worth noting that the reaction rate constants (k) of these plots for the production of methyl stearate in the present study were significantly higher and at lower temperatures than those reported for the tin zirconium oxide ($SnZr_h$) solid acid catalyst prepared using an ultrasonic-assisted hydrothermal method at temperatures from 80 °C up to 120 °C in the study by Ibrahim [40]. The (k) reaction rate constants reported in their study were 0.013 min^{-1}, 0.01467 min^{-1}, 0.01509 min^{-1} and 0.01565 min^{-1} at 80, 90, 100 and 120 °C, respectively [40].

Further discussion

A study of homogenous acid catalysts such as; sulfuric acid, phosphoric acid, perchloric acid and p-TSA on the esterification of oleic acid with oleyl alcohol with optimum reaction conditions of molar ratio 1:1, 3 h reaction time, 90 °C and 0.20 g of catalyst gave 93.88 % conversion to the ester product only for sulfuric acid, with lower conversions observed for the other catalysts [15]. In another study the highest yield (99 %) was obtained in the reaction of stearic acid with 1-butanol with an acid/alcohol/ catalyst (H_2SO_4) molar ratio of 1/15/0.75 and at a temperature 65 °C [3,51]. Our amidoximated PAN fibres as a protonated catalyst gave around 95.35 ± 4.09 % conversion to methyl stearate (GC-FID) analysis) using a molar ratio of methanol to acid of 35.5:1, 3hr reaction time and 3 g of PANF protonated catalyst in 26–27 mL at 90 °C,

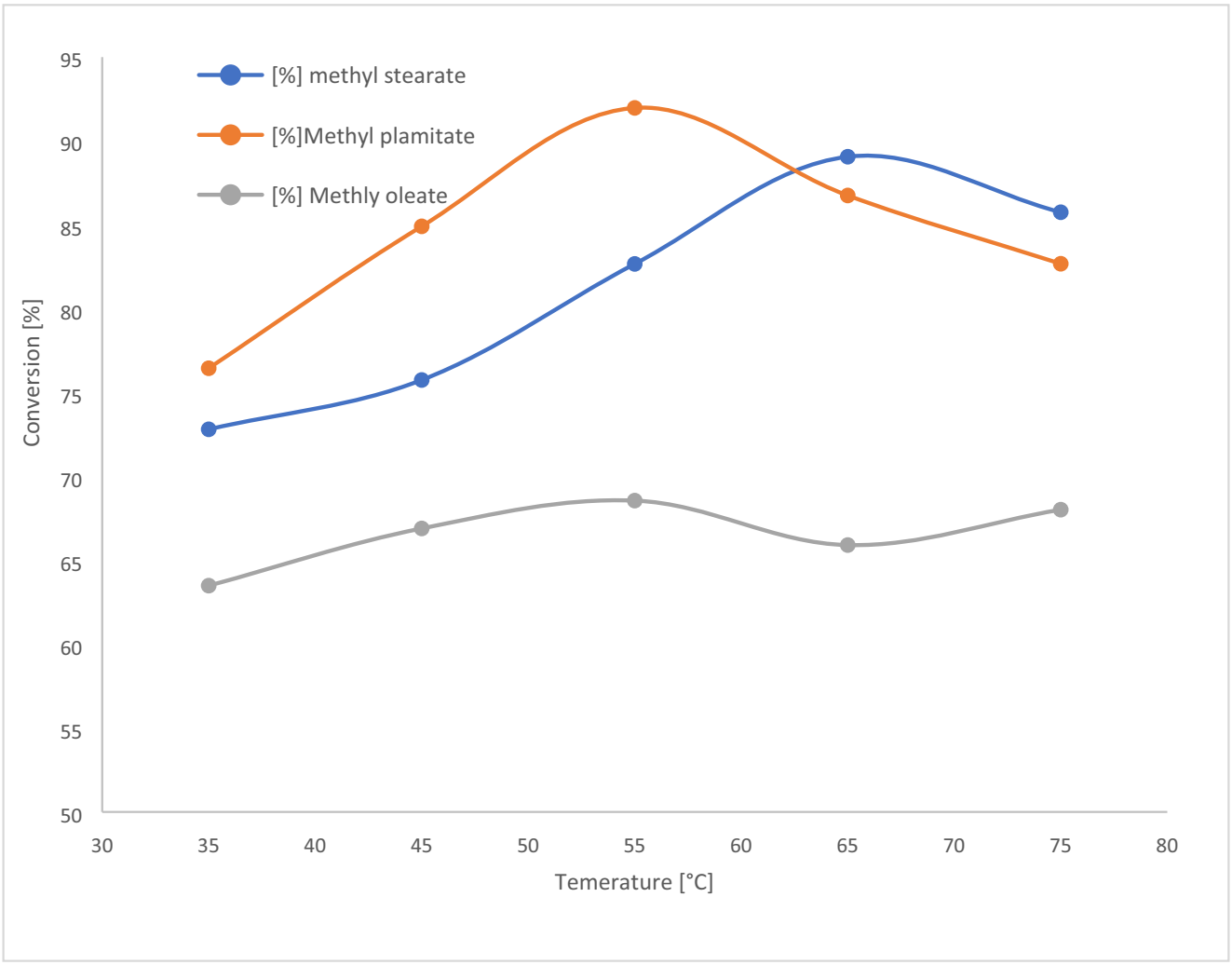

Fig. 14. GC-FID analysis for the formation of methyl stearate, methyl palmitate and methyl oleate as a function of temperature at reaction conditions. molar ratio of methanol to SA 87.7:1, methanol to PA 87.03:1 and methanol to OA 87.06:1, 3 h reaction time, 3 g of protonated catalyst, volume 26–27 mL.

which is similar to the conversions obtained with H_2SO_4 acid acting as catalyst.

Roman and his colleagues [27] used an ionic liquid as an acid catalyst (1-methylimidazolium hydrogen sulfate, [HMIM]HSO_4) for esterification of oleic acid with ethanol. Surface methodology (RSM) model was used to optimize the experimental conditions which were 95 % conversion to methyl oleate at 110 ± 2 °C, 8 h, 15:1 molar ratio of ethanol:oleic acid and 15wt.% catalyst [27]. Using a bismuth silicate catalyst, the esterification of oleic acid to methyl oleate achieved a conversion of about 90 %. The optimum esterification reaction conditions were: molar ratio of methanol to oleic acid 120:1, temperature 80 °C for 2hr over 0.3 g of bismuth silicate ($Bi_4Si_3O_{12}$ and Bi_2SiO_5) catalyst [49]. In comparison the catalytic activity of a sulfonated (CF-SO_3H) lignin-derived carbon fiber as heterogeneous solid acid catalyst was only reported for biodiesel production from oleic acid (molar ratio of methanol to oleic acid 10: 1) as feedstock. The highest conversion of oleic acid to its ester was 92 % in 4 h at 80 °C and the protonated catalyst retained high stability over 4 cycles of reuse [73].

Conventional cation ion-exchange resins, which offer sulfonic acid active sites, offer improved reusability and selectivity compared to homogenous catalysts in esterification reactions (See Table 7). Thus, the utilisation of resin-supported strong solid acids as replacements for traditional catalysts for production of biodiesel has increased over recent years. Notably, the sulphonated acidic ion exchange resin Amberlyst (Amberlyst types 15, 35, 46 and 70) which are effective, cheap, and green heterogeneous catalysts and have been widely established for esterification of free fatty acid [58]. However current literature now has many alternatives to these traditional polymer-based ion-exchange resins, for example mesoporous materials and ionomeric membranes for efficient esterification of FFAs [74].

It well known that the length of the alcohol chain and acid chain can have a hindering and slowing effect on the reaction rate [71]. In our experiment we used stearic acid, that is, a C18 fatty acid which has a longer carbon chain than the acids (acetic and propionic) in the esterification reactions using Smopex where 95–99 % conversion was achieved with butanol as shown in Table 7. Smopex is a fibrous solid acid catalyst, where PAN is grafted onto a polypropylene fibre and then the PAN is modified to incorporate ethylamine or N-substituted pyridine followed by treatment with HCl to create the acid catalyst.

The protonated amidoxime PAN fibres as a protonated catalyst have shown a unique behavior among all other catalysts available

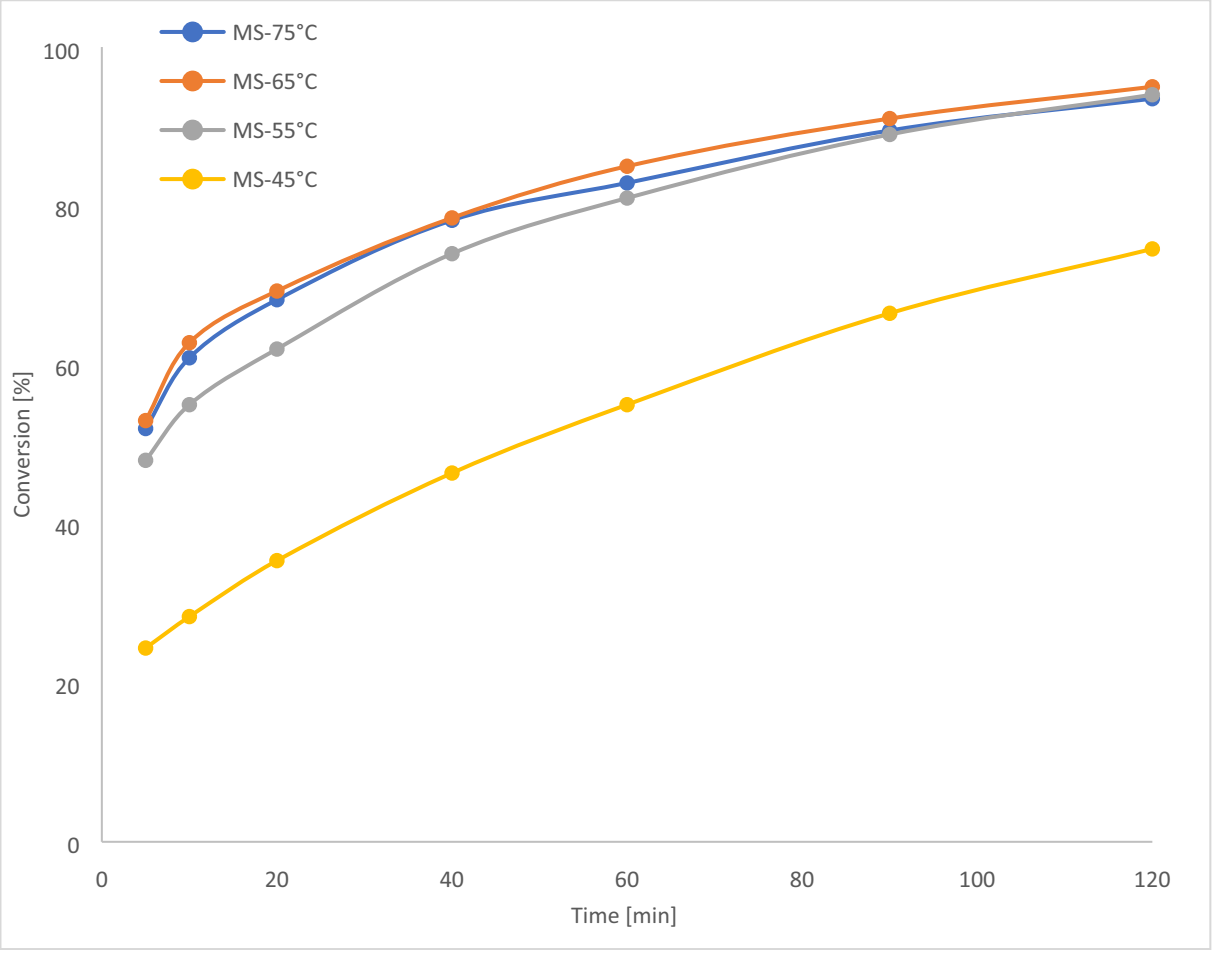

Fig. 15. GC-FID analysis for conversion of stearic acid to methyl stearate as a function of time at reaction condition. molar ratio of methanol to SA 87.7:1, 6 g of protonated catalyst total volume 109.52 ml.

for esterification, producing similar conversions to those obtained using a homogeneous strong acid catalyst but enabling reuse as well as recovery at the end of the process. The stability and reusability studies of the protonated catalyst revealed that the protonated amidoximated PANF catalyst can undergo multiple recyclability in stearic acid esterification without significant loss in activity. One of the advantages of using a fibrous catalyst in comparison to particulate catalysts is that they can be formatted as mesh or fabric. Thus, future work will incorporate the protonated catalyst of this work as a mesh in a novel rotating chemical contactor designed and tested for wastewater treatment at De Montfort University but which will be readapted for the continuous flow production of biodiesel from waste oils.

Conclusion

The protonated and crosslinked amidoximated PANF catalyst was shown to be an efficient acid catalyst in the esterification process with potential application for biodiesel production. Esterification reaction parameters of molar ratio of stearic acid to alcohol, reaction time, protonated catalyst concentration and temperature were chosen to optimize the synthesis of the methyl ester of stearic acid. A high percentage conversion (95.35 w/w%) was achieved at 90 °C with a molar ratio of methanol to stearic acid of 35.5:1, 3 h and 3 g of protonated catalyst in a total volume of 26–27 mL. A similar conversion of above 94 wt.% was achieved at the lower temperature of 65 °C but with a higher molar ratio of methanol to stearic acid of 87.7:1, at the lower reaction time of 2 h. Thus, the protonated PANF catalyst requires a relatively low temperature i.e., 65 °C, and only a comparatively short reaction time, that is 2 hours to achieve maximum conversion albeit at a higher methanol to stearic acid molar ratio. The amount of methanol is relatively high as its necessary to promote the forward reaction in the reversible esterification reaction. The excess methanol is usually recovered by evaporation/distillation for reuse in the next reaction batch and this method is feasible and economically acceptable for the industrial production of biodiesel. These conversions were equivalent to those obtained using sulphuric acid as homogeneous catalyst, yet at lower temperatures. They were also better than many other heterogeneous catalysts which were all either powders or resins in that again lower temperatures and shorter reaction times were used to achieve similar conversions. The network of PANF polymeric fibrils which make up the fibres of the catalyst mesh are also likely to adsorb/trap water formed in the reaction shifting the esterification equilibrium and improving conversion.

The protonated amidoximated PANF catalyst was batch recycled for 13 cycles before being regenerated. The ATR-FTIR spectra showed that after regeneration, the protonated catalyst was blocked with methyl stearate and that the amidoxime sites had been converted to amides which are more difficult to protonate.

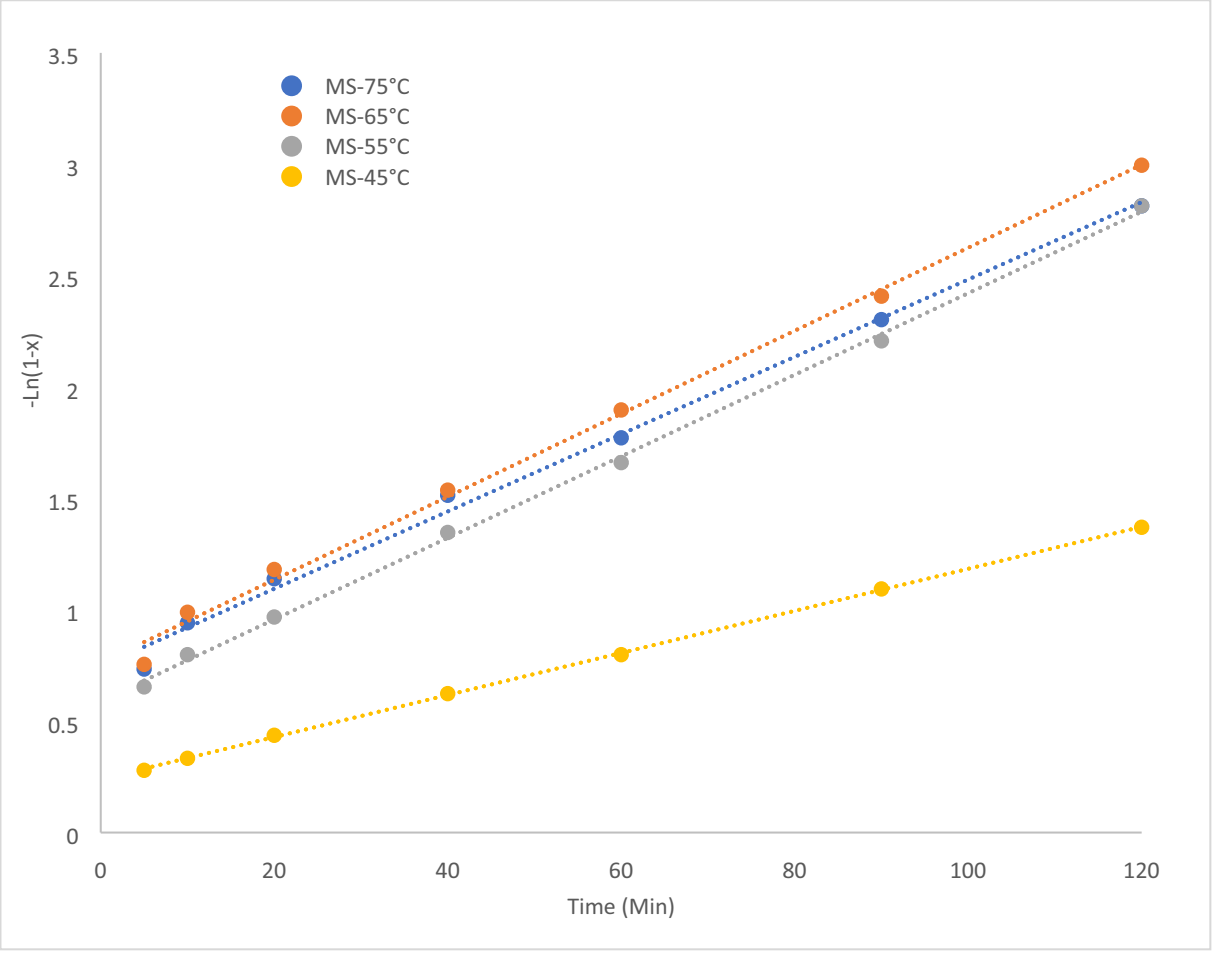

Fig. 16. Kinetic plots for the esterification of stearic acid to produce methyl stearate – Pseudo-first order, at reaction conditions; molar ratio of methanol to SA 87.7:1, 6 g of protonated catalyst at different temperatures, total volume 109.52 ml.

Photo 1. Esterification reaction under water-cooled reflux in Radley Carousel reactor.

To overcome this problem, washing the protonated catalyst with DCM more thoroughly prior to re-acidification and reuse would allow a truer evaluation of its potential for an effective in-situ regeneration.

Advantages of the protonated PANF catalyst mesh apart from its good efficacy and recyclability are that it can be used in a simple rotating disc continuous flow reactor with ease of use in comparison to homogeneous acids and heterogeneous powders and resin catalysts. It is produced at industrial quantities and all these advantages suggest that it has potential in esterification of FFAs and hence would be useful in biodiesel production from low value waste sources with high fatty acid content such as FOGs.

Table 6
Pseudo-first order kinetic results for esterification of stearic acid (SA) by methanol to methyl stearate (MS) using the protonated catalyst.

Pseudo-first order			
Samples	k, min^{-1}	R^2	Linear regression
MS-75 °C	0.0174	0.99	y = 0.0174x + 0.747
MS-65 °C	0.0186	0.99	Y = 0.0186x + 0.7622
MS-55 °C	0.0183	0.99	Y = 0.0183 + 0.5904
MS-45 °C	0.0094	0.99	Y = 0.0094x + 0.2398

Table 7
Comparison of the performance of heterogeneous catalysts in biodiesel production. Partially reproduced from Ahmed and Huddersman, 2022 [3].

Catalyst	Feedstocks	Esterification reaction conditions	yield %	Cycles	Ref.
A novel fibrous sulfated ZrO_2 (SO_4^{2-}/ZrO_2) acid cat.	Acetic acid	The n-butanol. acetic acid molar ratio 1.1:1, reaction temp.90 °C, 0.2 g cat., 1 h.	95–99 %	6 cycles	[75]
- A fibrous polymer-supported sulphonic acid (Smopex-101) -Amberlyst 15,	propanoic acid	The molar ratio of (1:1, 2:3, 3:2), 55–65 ∘C. reaction rate was higher for the fibre catalyst than with the Amberlyst 15. Second order 1.82×10^{-3} $dm^9/(mol^2\ g\ min)$ at 60 ∘C with the initial molar ratio 1:1 and 7.03×10^{-4} $dm^9/(mol^2\ g\ min)$ Amberlyst15.	NA Smopex-101 showed higher activity	4 cycles	[70]
-A fibrous polymer-support sulphonic acid, (Smopex-101) -Amberlyst 15, - HCl	Acetic acid Propanoic acid	acetic acid and ethanol (4:1, 2:1, 1:1, 1:2, 1:4), propanoic acid and methanol (1:1, 2:3, 3:2). at 60 ∘C, total vol.130 dm^3, 1–5 g of cat. Smopex-101 showed higher activity compared Amerlyst15, HCl.	Smopex-101 showed higher activity	NA	[71]
Amberlyst-15 (A-15) Amberlyst-35 (A-35) Amberlyst-16 (A-16) and Dowex HCR-W2	Free fatty acids (FFA) in waste cooking oil (WCO)	20 vol.% methanol with 10 g of FFA, at 50–60 °C with 1–2 wt.% catalyst, samples were taken at 3, 5, 10 min and every 20 min of reaction time.	A-15 > A-35 > A-16 >	NA	[76]
Amberlyst 70 ion exchange resin	FFA, propionic acid	Acid to alcohol molar ratios,1:2, 1:1, and 2:1, 80 °C up to 120 °C, and catalyst loadings (8.0, 4.0, and 0.8 wt. %, 150 min reaction time.	69–71 %	NA	[20]
Amberlyst-15	FFA. lauric, myristic, palmitic and stearic acid	Acid to methanol molar ratio 1:5, at 150 ∘C, 7 wt. % of cats.,400 min reaction time.	86 %	NA	[21]
Amberlyst 46	FFA. oleic acid	Methanol to Acid molar ratio 3:1, 100 °C, 15wt. % catalyst and 2 h reaction time.	96.8–98.3 %	10	[22]
Amberlyst-15	FFA. Acetic acid (AcOH)	Acid to ethanol molar ratio was 1. 4, at 70 °C, 4 mg of cat., at 90 min reaction time.	70 %	NA	[23]
Amberlyst −45	Vegetable oil, methanol, ethanol	Oil/alcohol molar ratio 1:18, with 10wt. % of catalyst at 170 °C, 360 min reaction time.	77.2 %	5cycle 70.2 %	[58]
Amberlyst-15 (A-15) Amberlyst-35 (A-36) Amberlyst-IR120 (A-IR120)	Sludge lipid from wastewater	In situ transesterification with sewage sludge as raw material. Amberslyst IR120/Sludge molar ratio 1:2, methanol/Sludge molar ratio 33:1, at 120 °C, 21 h.	32.9 % A-IR120	6 cycles	[77]
Sulphonated carbon-based solid acid catalysts	palm fatty acid distillate (PFAD)	catalyst loading of 4 wt.%, methanol-to-PFAD molar ratio of 15:1, temp. 65 °C and 1 h. the activity reduces in second cycle	94–95 %	4cycle 25 %	[78]

Note. All the Amberlyst resins are sulphonated resins.

Declaration of Competing Interest

The authors declare that they have no known competing financial interests or personal relationships that could have appeared to influence the work reported in this paper.

Acknowledgements

This work is supported by funding from the co-sponsors Daphne Jackson Trust, Society of Chemical Industry (SCI) and Royal Society of Chemistry (RSC), and hosted at De Montfort University, Leicester. WE also thank the technical team for their help with instrumentation, especially Dr. Ketan Ruparelia who ran the NMR instrumentation.

Reference

[1] A.P. Bora, D.P. Gupta, K.S. Durbha, Fuel 259 (2020).
[2] Tarigan J. Br., Ginting M., Mubarokah S.N., Sebayang F., Karo-karo J., Nguyen T. T., Ginting J. and Sitepu E. K., RSC Advances, 9 (2019), 35109.
[3] R. Ahmed, K. Huddersman, J. Ind. Eng. Chem. 110 (2022) 1–14.
[4] S. Semwal, A.K. Arora, R.P. Badoni, D.K. Tuli, Bioresour. Technol. 102 (2011) 2151–2161.
[5] [5] Srivastava N., Srivastava M., Gupta V. K., Manikanta A., Mishra K., Singh S., Singh S., Ramteke P. W., and Mishra P. K., 3Biotech, 8 (2018), 245.
[6] A.C. Dimian, A.A.J. Kiss, Clean. Prod. 239 (2019) 2–42.
[7] Bashira M.J.K., Wong L. P., Hilaire D. St., Kim J., Salako O., Jean M. J., Adeyemi R., James S., Foster T., Pratt L.M, J. Environ. Chem. Eng., 8(4), (2020), 103848.
[8] [8] Abomohra Abd El-F., Elsayed M., Esakkimuthud S., El-Sheekh M., Hanelt D., Prog. Energy Combust. Sci., 81(2020), 100868.
[9] J.M. Marchetti, A.F. Errazu, Biomass Bioenergy 32 (2008) 892–895.
[10] Khan Z., Javed F., Shamair Z., Hafeez A., Fazal T., Aslam A., Zimmerman W. B., Rehman F., J. Ind. and Eng. Chem., 103 (2021), 80–101.
[11] S. Ganesan, S. Nadarajah, X.Y. Chee, M. Khairuddean, G.B. Teh, Renewable Energy 153 (2020) 1406–1417.
[12] R. Sankaran, P.L. Show, J.-S. Chang, Biofuels Bioprod. & Biorefin. 10 (2016) 896–916.
[13] K.I. Doudin, Fuel 284 (2021).
[14] G. Jyoti, A. Keshav, J. Anandkumar, Int. J. Chem. React. Eng. 14 (2016) 2.
[15] Al-Arafi N., and Salimon J., E-, J. Chem. 9 (1) (2012) 99–106
[16] Z. Dastjerdi, M.A. Dubé, Environ. Prog. Sustain. Energy 32 (2) (2013) 406–410.
[17] G. Lawer-Yolar, B. Dawson-Andoh, E. Atta-Obeng, Sustain. Chem. 2 (1) (2021) 206–221.
[18] H.R. Mahmoud, S.A. El-Molla, M.M. Ibrahim, Renewable Energy 160 (2020) 42–51.
[19] Z.T. Alismaeel, A.S. Abbas, T.M. Albayati, A.M. Doyle, Fuel 234 (2018) 170–176.
[20] F. Leyva, A. Orjuela, D.J. Miller, I. Gil, J. Vargas, G. Rodríguez, Ind. Eng. Chem. Res. 52 (2013) 18153–18161.
[21] M. Banchero, G. Gozzelino, Energies 11 (2018) 1843.
[22] O. Ilgen, Fuel Process. Technol. 124 (2014) 134–139.
[23] M.H. Alhassani, S.M. Al-Jubouri, W.O. Noori, H.A. Al-Jendeel, Int. J. Eng. (IJE), IJE Trans. B: Appl. 31 (8) (2018) 1172–1179.
[24] V.V. Ishtchenko, K.D. Huddersman, R.F. Vitkovskaya, Appl. Catal. A: General 242 (2003) 123–137.
[25] E.A. Almadani, S.M. Radzi, F.W. Harun, Int. J. Appl. Chem. 12 (1) (2016) 62–67.
[26] W. Liu, P. Yin, X. Liu, S. Zhang, R. Qu, J. Ind. Eng. Chem. 21 (2015) 893–899.
[27] F.F. Roman, A.E. Ribeiro, A. Queiroz, G.G. Lenzia, E.S. Chaves, P. Brito, Fuel 239 (2019) 1231–1239.
[28] C. Song, Y. Qi, T. Deng, X. Hou, Z. Qin, Renewable Energy 35 (2010) 625–628.
[29] K. Saravanana, B. Tyagia, H.C. Bajaja, J. Indian, Chem. Sect. A 53 (7) (2014) 799–805.
[30] P. Prinsen, R. Luque, C. González-Arellano, Micropor. Mesopor. Mater. 262 (2018) 133–139.
[31] F. Ketzera, D. Celante, F. de Castilhos, Micropor. Mesopor. Mater. 291 (2020).
[32] Q. Zhang, T. Yang, D. Lei, J. Wang, Y. Zhang, ACS Omega 5 (22) (2020) 12760–12767.
[33] S.B. Neji, M. Trabelsi, M.H. Frikha, Energies 2 (2009) 1108–1117.
[34] Bassan I. A.L., Nascimento D. R., San Gil R. A.S., Pais da Silva M. I.,Moreira C. R., Gonzalez W. A., Faro Jr A. C., Onfroy T., Lachter E. R., Fuel Process. Technol., 106 (2013), 619-624.
[35] S.N. Rabelo, V.P. Ferraz, L.S. Oliveira, A.S. Franca, Int. J. Eviron. Sci. Dev. 6 (12) (2015) 964–969.
[36] T. Yuan, E. Akochi-Koble, D. Pinchuk, F.R. Van de Voort, Int. J. Renew. Energy Biofuel 2014 (2014) 1–13.
[37] M.A. Dube, S. Zheng, D.D. Mclean, M.J.A. Kates, J. Am. Oil Chem. Soc. 81 (2004) 599–603.
[38] C.F. Souza, M.T. Araujo, R.C. Santos, D.F. Andrade, B.V. Silva, L.A. Avila, Energy & Fuels 32 (2018) 11547–11554.
[39] K. Saravanan, B. Tyagi, H.C. Bajaj, J. Porous Mater. 23 (4) (2016) 937–946.
[40] S.M. Ibrahim, Renew. Energy 173 (2021) 151–163.
[41] M. Rosset, O.W. Perez-Lopez, Vib. Spectrosc. 105 (2019).
[42] N.G. Siatis, A.C. Kimbaris, C.S. Pappas, P.A. Tarantilis, M.G. Polissiou, J. Am. Oil Chem. Soc. 83 (2006) 53–57.
[43] F. Ezebor, M. Khairuddean, A.Z. Abdullah, P.L. Boey, Energy 70 (2014) 493–503.
[44] M. Satyanarayana, C.A. Muraleedharan, Energy 36 (4) (2012) 2129–2137.
[45] B.B. Uzun, M. Kılıç, N. Özbay, A.E. Pütün, E. Pütün, Energy 44 (1) (2012) 347–351.

[46] N. Rasimoglu, H. Temur, Energy 68 (2014) 57–60.
[47] W. Wang, F. Li, Y. Li, Green Process. Synth. 8 (1) (2019) 776–785.
[48] T. Xincheng, N. Shengli, J Ind Eng Chem. 69 (2019) 187–195.
[49] H.R. Mahmoud, Fuel 256 (2019).
[50] B.D. Naik, M. Udayakumar, Mater. Today: Proc. 46 (2021) 9855–9861.
[51] V. Kastratovic, M. Bigovic, Chem. Ind. Chem. Eng. Q. 24 (3) (2018) 283–291.
[52] [52] Fogler H.S., Elements of Chemical Reaction Engineering, 4th ed., Upper Saddle River, (2006), NJ 07458 Westford, Massachusetts.
[53] H. Zhang, J. Ding, Z. Zhao, Bioresour. Technol. 123 (2012) 72–77.
[54] Mo X., López D.E., Suwannakarn K., Liu Y., Lotero E, J Goodwin J. G., J. Catal., 254 (2008) 332–338
[55] K. Ngaosuwan, J.G. Goodwin, P. Prasertdham, Renew. Energ. 86 (2016) 262–269.
[56] N. Shibasaki-Kitakawa, H. Honda, H. Kuribayashi, T. Toda, T. Fukumura, T. Yonemoto, Bioresour. Technol. 98 (2007) 416–421.
[57] H. Zhang, F. Tain, L. Xu, R. Peng, Y. Li, J. Deng, Chem. Eng. J. 388 (2020).
[58] N.M. Cabral, J.P. Lorenti, W. Plass, J.M.R. Gallo, Front. Chem. 8 (2020) 305.
[59] [59] Ghorbani–Choghamarani A., Taherinia Z. & Tyula Y. A., Scientific report, March 2022, Vol.12, (2022), 10338, www.nature.com/scientificreports.
[60] C.A. Akinremi, S. Rashid, P.D. Upreti, G.T. Chi, K. Huddersman, RSC Adv. 10 (22) (2020) 12941–12952.
[61] G.T. Chi, K.D. Huddersman, J. Adv. Oxid. Technol. 14 (2) (2011) 235–243.
[62] Y. Liu, E. Lotero Jr., J.G. Goodwin, J. Catal. 243 (2006) 221.
[63] V. Kastratovic, M. Bigovic, Chem. Ind. Chem. Eng. Q. 24 (3) (2018) 283–291.
[64] S.B. Neji, M. Trabelsi, M.H. Frikha, Energies 2 (2009) 1107.
[65] D. Arcens, E. Grau, S. Grelier, H. Cramail, F. Peruch, Eur. J. Lipid Sci. Technol. 122 (4) (2020) 1900294.
[66] K. Srilatha, N. Lingaiah, P.S.S. Prassard, B.L.A.P. Devi, R.B.N. Prassard, S. Venkateswar, Ind. Eng. Chem. Res. 48 (2009) 10816.
[67] W. Hong-hong, L. Li-jun, G. Shu-wen, J. Fuel Chem. and Technol. 45 (3) (2017) 303–310.
[68] Zhang Y., Cortez J. C., Hammer S. K., Carrasco-Lopez C., Echauri S. A. G., Wiggins J. B., Wang W., Avalos J. L., Nat. Commun., 13(1),2022, 270.
[69] P. Mäki-Arvela, T. Salmi, M. Sun-dell, K. Ekman, R. Peltonen, J. Lehtonen, Appl. Catal. A 184 (1999) 25–32.
[70] [70] Lilja J, Aumo J, Salmi T, D. Yu. Murzin, Mäki-Arvela P, Sun-dell M, Ekman K, Peltonen R, Vainio H., Appl. Catal. A, 228(2002),253–267.
[71] Lilja J, D. Yu. Murzin, Salmi T, Aumo J, Mäki-Arvela P, Sun-dell M., J. Mol. Catal. A, 182–183(2002),555–563.
[72] Wu L., Hu X.,Wang S., Hasan M. D. M, Jiang S., Li T., Li C-Z., Fuel, 212 (2018), 412–421
[73] S. Adhikari, Z. Hood, N. Gallego, C. Contescu, MRS Adv. 3 (47–48) (2020) 1–9.
[74] V. Trombettoni, D. Lanari, P. Prinsen, R. Luque, A. Marrocchi, L. Vaccaro, Prog. Energy Combust. Sci. 65 (2018) 136–162.
[75] Y. Liaoa, X. Huang, X. Liaoa, B. Shi, J. Mol. Catal. A: Chem. 347 (2011) 46–51.
[76] N. Ozbay, N. Oktar, N.A. Tapan, Fuel 87 (2008) 1789–1798.
[77] Y. Patino, L. Faba, E. Díaz, S. Ordonez, J. Water Process Eng. 44 (2021).
[78] M.S.M. Farabia, M.L. Ibrahimd, U. Rashid, Y.H. Taufiq-Yap, Energy Convers. Manag. 181 (2019) 562–570.